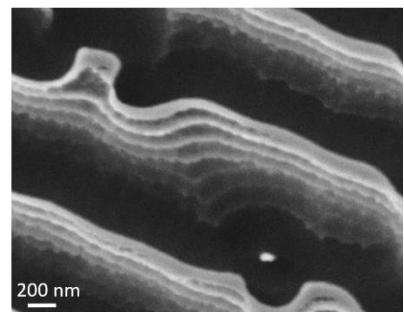
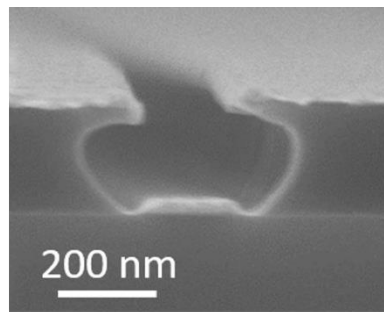
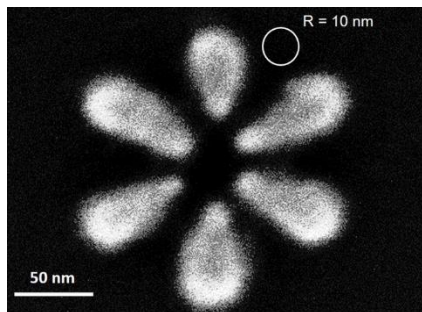


NanoFrazor Recipe Book



Preface

Already before the installation of the first NanoFrazor instrument at a customer's site in 2014 it has been clear that in order for the technology to be competitive in the lithography market, all the related sample processing has to be as straightforward as possible. Ideally, the adopters of NanoFrazor technology should be able to use their existing nanofabrication processes and materials with as little modifications as possible in order to achieve a smooth transition to the new technology. Therefore, developing pattern transfer processes that both take full advantage of the potential of the NanoFrazor and at the same time introduce as little changes to the user's existing processes has been our guiding principle.

This book summarizes the processing knowhow we have gathered into a single text that we hope will act as a useful reference for all NanoFrazor users in their pattern transfer processes. This book will not, however, replace our direct support to our customers and we will remain available to help with any processing and patterning related questions also in the future.

We would like to thank all (present and past) members of the Heidelberg Instruments Nano · SwissLitho-team for their contributions towards the contents of this book and the development of the technology in general. We are also grateful of the longstanding and close collaboration with the members of the Nanofabrication group at IBM Research – Zurich, in particular Dr. Armin Knoll and Dr. Heiko Wolf.

Finally, we take this opportunity to thank our academic and industrial collaborators for providing the motivation and inspiration to develop the various processes and materials to enable their applications and for allowing us to share the images of the results.

The Authors

June 25, 2020



Table of contents

1	Selecting the right pattern transfer process.....	5
1.1.	Bilayer lift-off (BLO)	5
1.2	High resolution lift-off (HRLO).....	6
1.3	High resolution etch (HRE).....	7
1.4	3D structuring resists & replication (3DP).....	8
1.5	3D and deep etch into hard materials (3DT).....	9
2	Resists and materials	10
2.1	Thermal resists	10
2.1.1	Polyphthalaldehyde (PPA).....	11
2.1.1.1	Preparation and storage of PPA solutions.....	12
2.1.2	Other thermal resists.....	13
2.2	Materials for pattern transfer, wear reduction, thermal shielding etc.....	14
2.2	Spin-coating.....	15
2.3.1	Spin-coating theory	15
2.3.1.1	Considerations with respect to achieving accurate overlay	16
2.3.2	Calibrating film thicknesses	19
2.3.3	Improving resist adhesion	20
3	Standard NanoFrazor processes.....	21
3.1	Bilayer lift-off.....	21
3.1.1	Introduction to bilayer lift-off.....	21
3.1.2	Lift-off resists and their properties.....	22
3.1.3	Sample pre-treatment	22
3.1.3.1	HMDS adhesion promoter.....	23
3.1.4	Notes on patterning	24
3.1.5	Descum, developing, lift-off.....	25
3.1.5.1	Using a PMGI underlayer.....	25
3.1.5.2	Using a PMMA/MA underlayer.....	27
3.1.6	Notes on the possibilities and limitations of the process	28
3.2	High-resolution pattern transfer with a silicon hard mask.....	29
3.2.1	Introduction to high-resolution pattern transfer	29
3.2.2	Sample pre-treatment	31
3.2.3	Preparation of the pattern transfer stack.....	32
3.2.3.1	Evaluating hard mask quality.....	33

3.2.3.2	Notes on patterning high-resolution stacks	34
3.2.3.3	Etching the PPA and the hard mask.....	35
3.2.4	High-resolution lift-off.....	37
3.2.4.1	Opening the stack, lift-off	37
3.2.4.2	Notes on the possibilities and limitations of the process.....	39
3.2.5	High-resolution etching	41
3.2.5.1	Opening the stack, etching, removal of the stack.....	41
3.2.5.2	Notes on the possibilities and limitations of the process.....	42
3.3	3D structuring resists & replication	43
3.3.1	Introduction to 3D pattern transfer	43
3.3.2	Some practical recommendations for 3D patterning.....	44
3.3.3	Soft moulding from resist and nanoimprint lithography	45
3.3.4	Replicating metals from 3D resist templates	48
3.3.5	Notes on the possibilities and limitations of the process.....	50
3.4	3D etching into hard materials.....	51
3.4.1	Introduction to 3D etching	51
3.4.2	Reactive ion etching 3D structures into Si and SiO _x	52
3.4.3	Amplified reactive ion etching with hard masks.....	54
4	Non-standard processes for pattern transfer	56
4.1	SIS – Sequential Infiltration Synthesis for high-resolution pattern transfer.....	56
5	Notes on relevant processing techniques and materials	58
5.1	Reactive ion etching.....	58
5.2	Ion beam etching.....	59
5.3	Wet etching.....	60
5.4	Working with 2D materials.....	61
6	References.....	63
7	Appendices:	65
	Appendix 1: Spin-tables for various resists and pattern transfer materials.....	65
	Appendix 2: Solvent compatibility of PPA.....	67
	Appendix 3: Selected reactive ion etching recipes, etch rates and selectivities	68

1 Selecting the right pattern transfer process

A range of pattern transfer processes matching the requirements of different geometries and materials have been developed or adapted for the NanoFrazor. This section provides a quick selection guide for choosing the right process for your application.

1.1. Bilayer lift-off (BLO)

When to use the bilayer lift-off process:

- You want to pattern an evaporated thin film of material AND
- The smallest features of your pattern are larger than ~100 nm OR
- The layer directly under the resist is sensitive to oxygen plasma exposure.

The process is especially useful for creating high-quality electrical contacts. The process flow is presented in Figure 1. See Chapter 3.1 for an in-depth discussion of the process.

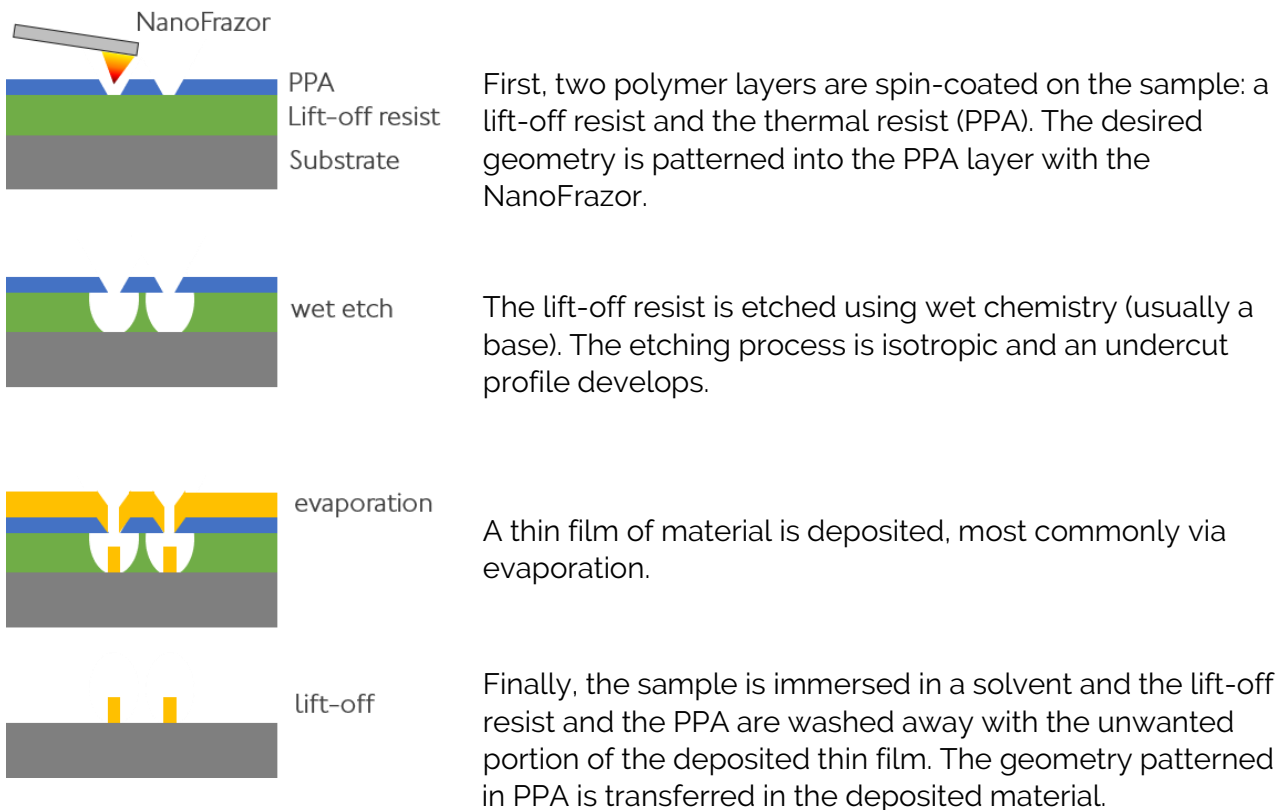


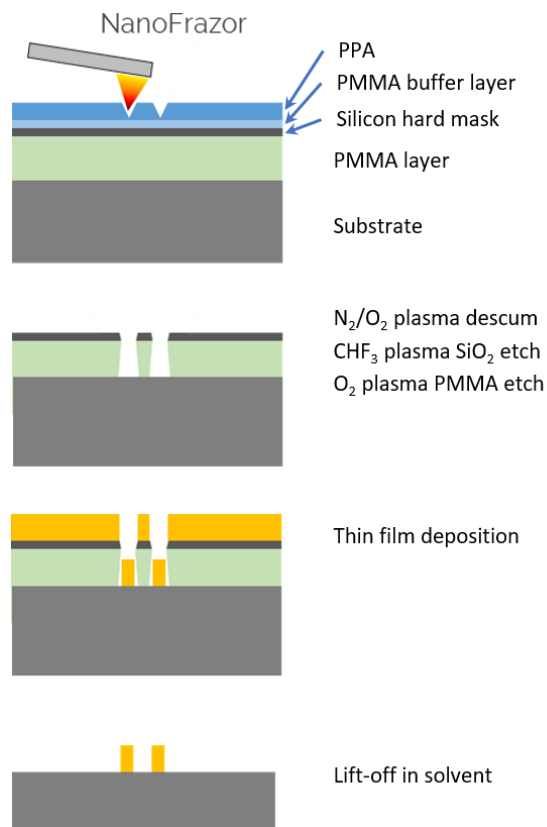
Figure 1 Bilayer lift-off process.

1.2 High resolution lift-off (HRLO)

When to use the high-resolution lift-off process:

- You want to pattern an evaporated thin film of material AND
- The smallest features of your pattern are smaller than ~100 nm AND
- The layer directly under the resist is not sensitive to oxygen plasma exposure.

High-resolution lift-off process flow is presented in Figure 2. Chapter 3.2.5 discusses the process in more detail.



A lift-off stack comprising a layer of sacrificial resist (typically PMMA), a silicon hard mask, a PMMA buffer layer (optional) and the PPA is spin-coated on the sample. The PPA layer is patterned with the NanoFrazor.

The PPA pattern is etched into the stack by reactive ion etching:

- 1: Descum to remove PPA (and PMMA) residues
- 2: SiO₂ etch with CHF₃
- 3: PMMA etch with O₂ plasma

A thin film of material is deposited, most commonly via evaporation.

The sample is immersed in a solvent and the residual pattern transfer stack is washed away with the unwanted portion of the deposited thin film.

Figure 2 High-resolution lift-off process.

1.3 High resolution etch (HRE)

When to use the high-resolution etch process:

- You want to etch a 2D pattern into the substrate under the resist.

Significant amplification of the initial PPA pattern depth is possible by tuning the selectivity of the dry etching process. For even higher depth amplification an intermediate hard mask layer (e.g. SiO₂) can be added. The pattern can be transferred into this layer before finally etching it into the substrate. See Figure 3 for the process flow and Chapter 3.2.6 for a detailed description of the process.

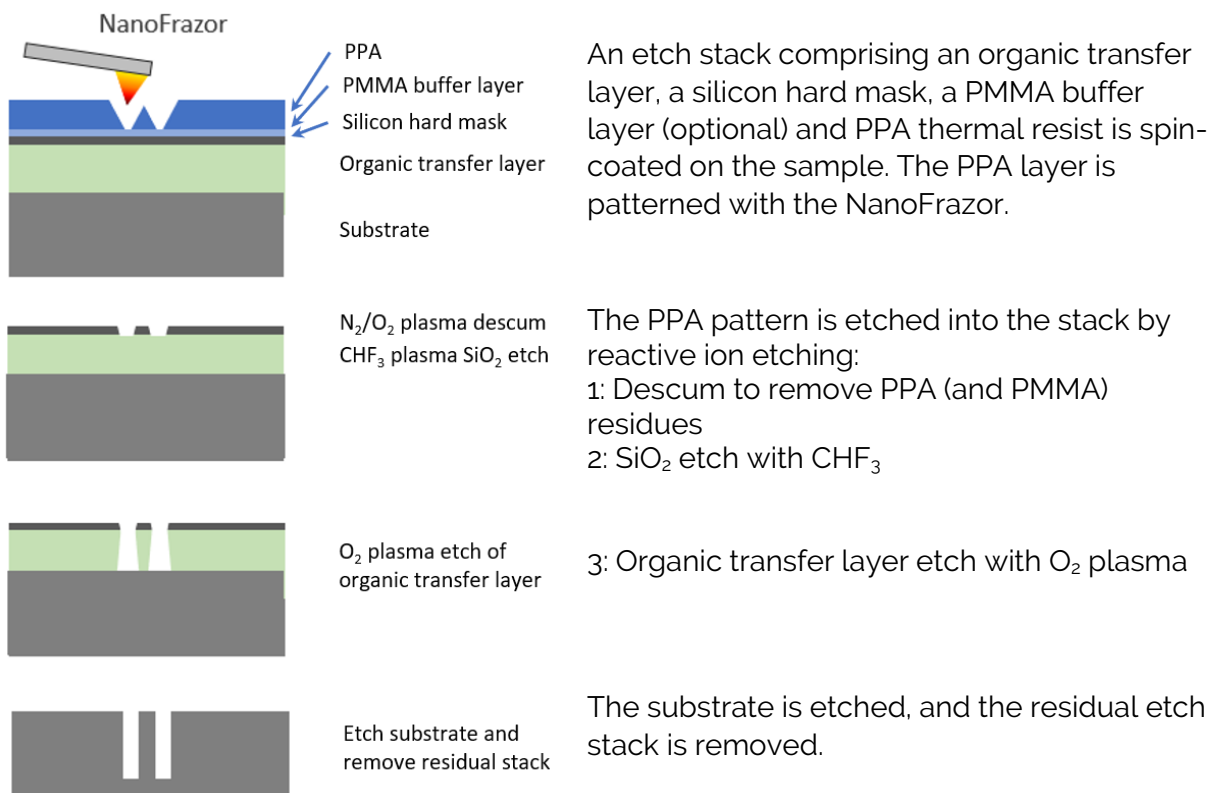


Figure 3 High-resolution etching process.

1.4 3D structuring resists & replication (3DP)

The unique 3D patterning capabilities of the NanoFrazor can be harnessed to production of 3D nanoimprint lithography masters or moulds; e.g., for electroless plating. Fabrication of sub-nm-accurate 3D shapes is possible, but the maximum depth of the patterns in the resist is limited to about 250 nm due to tip geometry. Figure 4 shows the 3D structure replication process flow and Chapter 3.3.4 describes the process in detail.

Process flow

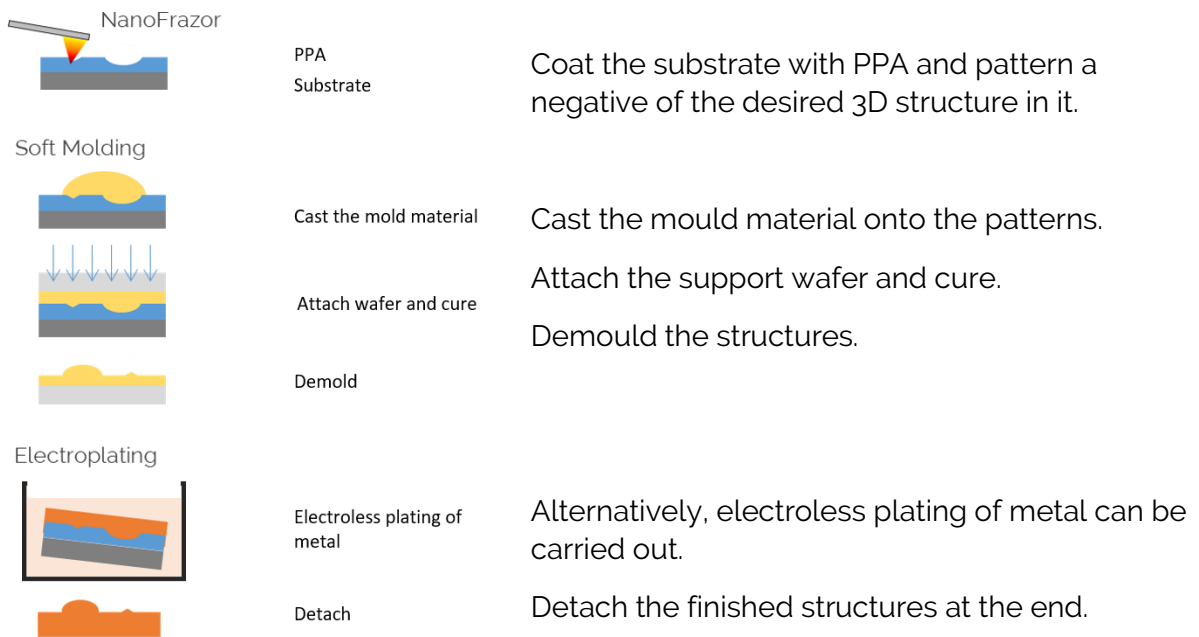


Figure 4 3D replication from resist patterns.

1.5 3D and deep etch into hard materials (3DT)

The 3D patterns written with the NanoFrazor can also be transferred to the substrate – and the depth of the patterns amplified - by etching. An optional intermediate hard mask layer helps in achieving an even stronger amplification of the pattern depth. Figure 5 shows the process flow for 3D transferring and Chapters 3.4.2 and 3.4.3 contain detailed descriptions of the process without an intermediate layer and with it, respectively.

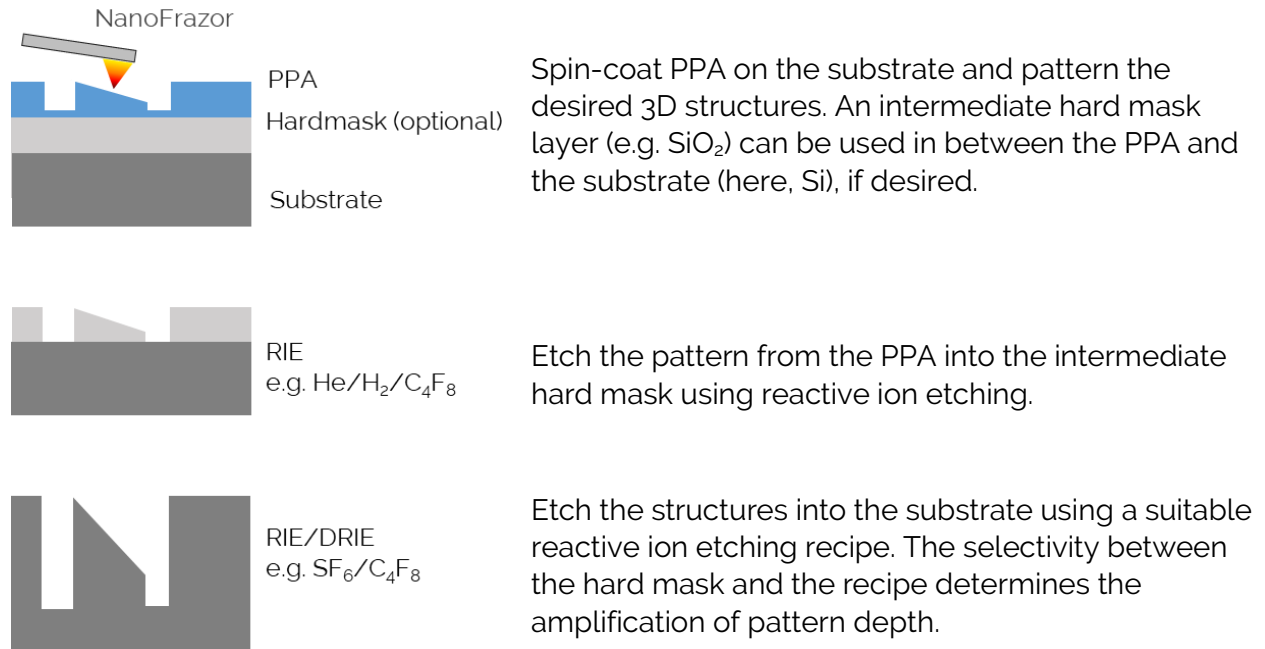


Figure 5 3D etching structures into substrates.

2 Resists and materials

The term **resist** is often used in the context of micro- and nanofabrication as an organic material that can be deposited onto a substrate and is susceptible to external stimuli such as electromagnetic radiation (UV, EUV, VIS etc.), particle beams (ions, electrons), heat and other mechanical or chemical inputs.

In addition, one often separates the resists into "positive resist" or "negative resist." In the case of a positive resist, the exposed areas (target design) are removed. Negative resists form a stable (cross-linked) material upon exposure; therefore, the not-exposed area (the negative of the target design) is removed.

2.1 Thermal resists

A "positive thermal resist" in the scope defined above is susceptible to heat and is removed from the areas exposed to sufficient heating.

The elevated temperature, here referred to as the heat trigger either softens the polymer above its glass transition point, enabling a plastic deformation (indentation) or it directly sublimates the material from solid into gaseous state, see Figure 6 below. Whereas indentation creates unwanted "pile-up" and limits choice of pattern geometries, sublimating the polymer directly into its volatile monomers ideally will not leave any residues.

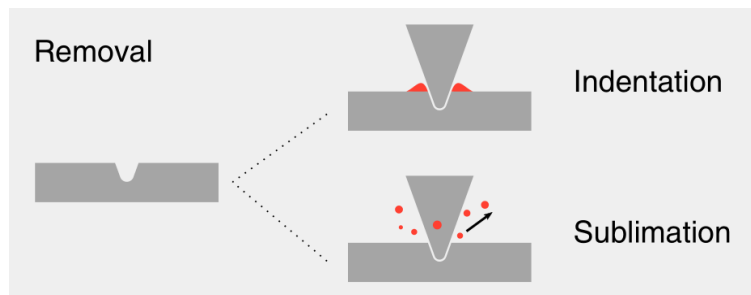


Figure 6 A schematic presentation of the two ways of removing material with a heated tip. In practice, both ways are often present simultaneously. [17]

2.1.1 Polyphthalaldehyde (PPA)

With regards to an optimal positive thermal resist, high sensitivity to heat is key. Polyphthalaldehyde (PPA) is the current gold standard for thermal scanning probe lithography (t-SPL). It has a very low ceiling temperature of $\sim -40^{\circ}\text{C}$, which explains its strong tendency to decompose into its monomers [18].

PPA demonstrates self-amplified decomposition (complete unzipping of the polymer backbone upon a single heat-triggered bond break [19]). Furthermore, the unzipping reaction is endothermic (consumes energy), which results in highly localized decomposition (low lateral heat spread) [20].

Macroscopically, the decomposition temperature of pure PPA ($T_{\text{dec}} \sim 180^{\circ}\text{C}$) lies in the same range as its glass transition temperature ($T_g \sim 180^{\circ}\text{C}$) [21]. Therefore, once the chains get mobile, they start to decompose into volatile monomers.

PPA also shows sufficient storage stability. The polymer is stable in solution in a refrigerator ($+5^{\circ}\text{C}$) for >3 months, as powder in a freezer (-18°C) for >1 year. Please refer to section 2.1.1.1 for more details on preparation and storage of PPA solutions.

Finally, PPA can be spin-coated in a broad thickness range of 2 nm to 10 μm , shows sufficient adhesion to most substrates and other resists, has a reasonable resistivity towards dry etching processes and is commercially available from the company Allresist.

2.1.1.1

Preparation and storage of PPA solutions

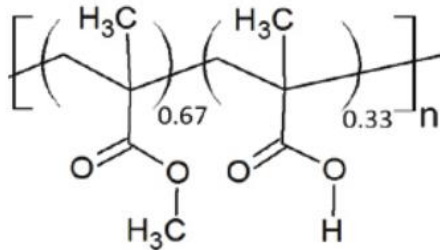
PPA is commercially available from the company Allresist under the product name [Phoenix 8100](#), and it is delivered as a powder. It must be dissolved in a solvent (anisole works best in most cases) prior to use, and the resulting concentration affects the thickness of the PPA films obtained via spin-coating. See Appendix 1 for the spin-speeds and concentrations required for different PPA thicknesses. A few general guidelines for handling the PPA powder and for preparing the solutions apply:

- Prepare the PPA solution in a glass vial with a PTFE sealed cap. Use only glass or PTFE pipettes for preparation of the solutions to avoid any contamination from the equipment used.
- Use an accurate enough balance for measuring the right amount of PPA powder (use weighing paper or similar). Then put the PPA powder in a glass vial and add the desired amount of anisole (density = 0.995 g/ml).
- In order to ensure that all the PPA powder is dissolved, the mixture must be shaken well, ideally at least 15 min on a mechanical shaker, if one is available.
- The undissolved (if any) PPA powder should be removed by filtering the solution into a fresh glass vial. A $\leq 0.2 \mu\text{m}$ PTFE filter is recommended. The filtering step should be executed even if no readily visible undissolved PPA is observed.
- After preparation, the solution should stand still for at least one hour before spin-coating. This allows for any small air bubbles generated during the filtering process to rise to the surface.
- Ready solution should be stored in a fridge (about 5 °C) and allowed to warm up to room temperature (about 15 min) before opening the vial. This helps avoid water condensation on the inside of the vial.
- The leftover powder should be stored in a freezer (-18 °C or colder) in order to maximize its lifetime. Note that the powder should be sealed in an airtight container (to avoid any water condensation during freezing or rewarming to room temperature). Allow the powder to warm to room temperature (at least 1 hour) before opening the airtight packaging. This prevents water condensing from the ambient air from contaminating the powder.

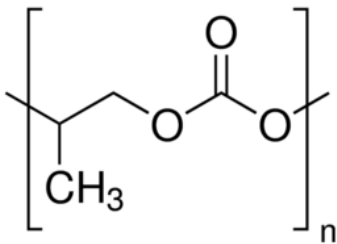
2.1.2 Other thermal resists

Even though we strongly recommend using PPA as the thermal resist for the NanoFrazor, a variety of other thermal resists have been explored, as well:

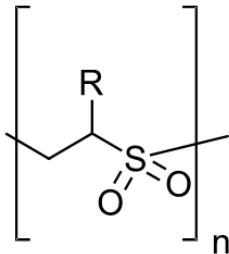
1. **PMMA-co-MA**, commercially available from Allresist ([AR-P 617 series](#)) [6]



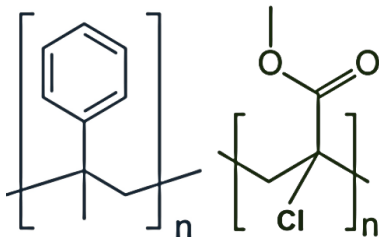
2. **Polypropylene Carbonate PPC** [15]



3. **Poly(olefin sulfones)**, very suitable for patterning due to low ceiling temperatures but less resistant to dry etching than PPA [16]



4. **CSAR 62**, commercially available from Allresist ([AR-P 6200](#)), for certain high resolution process, when PPA intermixing or dissolution occurs.



5. More exotic material systems usually show very high tip contamination and therefore significantly reduced tip lifetime.

2.2 Materials for pattern transfer, wear reduction, thermal shielding etc.

Apart from the thermal resist materials that can be removed by the hot tip, several other materials are needed for successful pattern transfer. A very short overview of the materials is given here, and the use of each respective material is described in detail where the material is applied in the process.

PMMA (polymethyl methacrylate), *AR-P 672 series, Allresist GmbH*

- Transfer layer for high-resolution lift-off.
- Ultra-thin (~2 nm) mechanical buffer layer for high-resolution patterning.
- Ultra-thin (~2 nm) thermal insulator layer for 3D patterning and etching.

SH 113 (silicon hardmask), *PiBond Oy*

- Ultra-thin (~1.5 nm), pinhole-free siloxane polymer layer that oxidizes into a silicon dioxide hard mask upon exposure to oxygen plasma. Used for high-resolution lift-off and etching processes.

OTL 405 (organic transfer layer), *PiBond Oy*

- Highly cross-linked, carbon-rich polymer transfer layer with improved etch resistance for high-resolution etching process.

PMGI (polymethylglutarimide), *SFG S -series, Kayaku Advanced Materials, Inc.*

- Slow-developing (~1 nm/s) lift-off resist for bilayer lift-off process that can be removed without residuals.

PMMA/MA (polymethyl (methacrylate-co-methacrylic acid)), *AR-P 617 series, Allresist GmbH*

- Originally an electron beam resist but develops also without exposure to electron beam, also in nonaqueous solvents making it a useful lift-off resist for the bilayer lift-off process.

2.2 Spin-coating

2.3.1 Spin-coating theory

In general, the thickness of a spin coated film is proportional to the inverse of the spin speed squared as in the below equation, where t is the thickness and w is the angular velocity given in revolutions per minute (rpm):

$$t \propto \frac{1}{\sqrt{\omega}}$$

We see from the equation that a film that is spun at four times the speed will be half as thick. Since several additional factors such as the specific solvents in the resist, the vapor pressure, and local temperature and humidity values (as well as variations) can affect the resulting film thickness, it is important to calibrate the film thickness as described in Section 2.3.2.

Despite the variations, spin curves depicting the expected film thickness as a function of the spin speed provide excellent guidance when working with a new or unusual resist material. The spin curves for the thermal resists and further materials used in our pattern transfer processes are included in Appendix 1.

2.3.1.1 *Considerations with respect to achieving accurate overlay*

NanoFrazor is capable of non-invasive imaging of sample topography and can be used for very accurate overlay of patterns over existing features on the sample. If a sample has any existing topography features on it, these will be detected on the topography in the resist layer spin-coated on top of the sample, as shown in Ref. 1. This enables aligning patterns with features under the resist with an overlay error of below 3 nm without the need to add any artificial marker structures on the sample in a separate processing step – the structures to be aligned will also act as alignment marks.

Good prediction of the residual topography on the resist surface is obtained by convolving the buried topography with a Gaussian shape and by inserting the employed Gaussian's width σ and amplitude R into the transfer Kernel:

$$K_{\tau} \simeq \frac{R}{\sigma^2 2\pi} e^{-\frac{(x^2+y^2)}{2\sigma^2}} \quad [1]$$

Typical values for σ and R would be 80 nm and 0.7, respectively. For more information on predicting the amplitude of residual topography over the resist, the reader is referred to Ref. 1. Importantly, the resist thickness does not influence the amplitude of residual topography to a great degree – single-atom thick MoS₂ flakes are easily visible through a 220-nm-thick resist layer, for example [2]. Figure 7a explains the formation of the residual topography in the resist: the topography emerges in an initially flat film due to capillary driven flow of material during solvent evaporation. Figure 7b shows an AFM image of an InAs nanowire with a diameter of 27 nm on a silicon substrate while Figure 7c shows the same nanowire after 61 nm PPA has been spin-coated on it. The residual topography is 2.9 nm and allows for easy detection and overlay of the nanowire.

A simple method of enhancing the contrast of topographies buried under resist surfaces was also presented in Ref. 1. Namely, faster solvent evaporation process results in a narrower and sharper profile of the residual topography making it easier to detect with the NanoFrazor. Exposing the resist film to a saturated vapour of highly volatile solvent dichloromethane for several minutes and allowing it to dry resulted in an improved contrast of the residual topography making it easier to overlay with the NanoFrazor (Figure 7d).

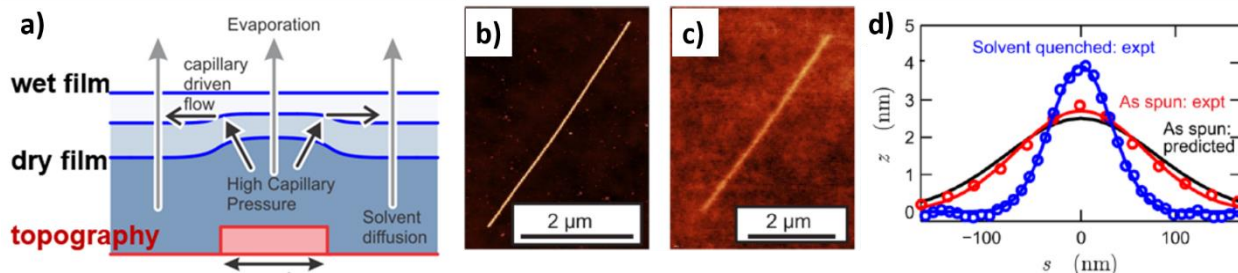


Figure 7 a) A schematic of the temporal evolution of resist free surface during different stages of the film coating process. The initially flat surface develops a residual topography vertically aligned with the structures underneath during solvent evaporation. b) Atomic force microscope image of an InAs nanowire ($d = 27$ nm) on a silicon surface. c) The same nanowire as in b) coated with a 61-nm-thick PPA layer. The residual topography has a height of 2.9 nm. d) The predicted (black solid line) and experimentally measured (open circles) profiles of the nanowire in c) before (red) and after exposure of the film to a dichloromethane saturated atmosphere (blue). Adapted from Ref. 1.

Some examples of the residual topography amplitude over a resist film are given in Table 1 below. Nanowires down to a 10 nm diameter as well as single-atom thick 2D material flakes and individual small nanoparticles can be easily detected (and overlaid) with the NanoFrazor. Single-walled carbon nanotubes (SWNTs), however, do not produce a significant residual topography over the resist film and therefore cannot be detected with the tool. However, accurate alignment to SWNTs has been demonstrated by first locating them by AFM (see Figure 8a) and including any thick SWNT bundles, catalyst particles or other existing and recognizable topography nearby in the image. These additional features can act as “natural markers” or points of reference of the SWNT’s exact location and a very accurate overlay can be achieved (Figure 8b).

Table 1 Examples of residual topography amplitude for selected nanostructures under 80-nm-thick PPA layer.

$R = 0.7$ $\sigma = 80$ nm	Width	Height	Residual topography
Single-walled carbon nanotube	$\varnothing 0.5 - 1$ nm	0.5 - 1 nm	< 0.005 nm
Nanowire	$\varnothing 10$ nm	10 nm	0.45 nm
Single-layer MoS ₂ flake	> 1 μ m	0.65 nm	0.45 nm
Nanoparticle	$\varnothing 25$ nm	25 nm	0.45 nm

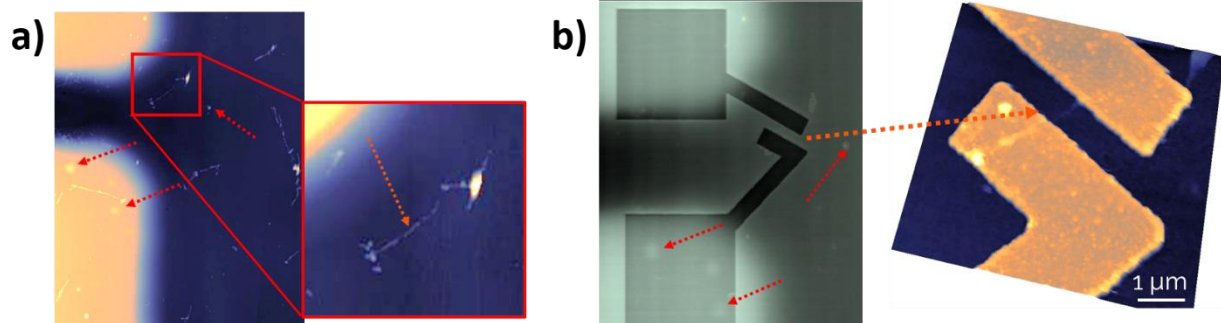


Figure 8 a) Accurate overlay to an individual single-walled carbon nanotube is possible by first imaging it on its original substrate and including any characteristic nearby topography in the image (here, e.g. the electrodes fabricated by photolithography, dirt particles) and using these as natural markers in the overlay process. b) The nanotube in a) after the patterning (left) and after metal lift-off (right). Sample provided by Prof. Tai-Cheng Lee, National Taiwan University.

2.3.2 Calibrating film thicknesses

We strongly recommend using an atomic force microscope (AFM) for accurately measuring the thicknesses of the thin spin-coated polymer films. Once the film has been spin-coated and soft-baked, draw a scratch on it using either sharp-tipped plastic tweezers or a sharp, flexible metal needle. Using such tools will prevent scratching into the substrate material underneath (e.g. silicon, silicon dioxide) which could distort the measurement result.

Find a clean location along the scratch and scan it with the AFM (see Figure 9, left). Level the image carefully in an AFM image processing software (e.g. Gwyddion) and measure the film thickness. If the profile is very clean (see Figure 9, right), only one measurement per sample is enough.

Alternatively, profilometer can be used for measuring somewhat thicker polymer films (> 100 nm) as a quick check of the spin-coated film thicknesses. However, as profilometer measurements tend to be noisy, we don't recommend using them for estimating absolute film thicknesses.

Finally, ellipsometry can offer a quick, non-invasive way of measuring the thicknesses of polymer films. However, in order to achieve reliable results with ellipsometry, the optical properties of the polymer must be very precisely known and when a stack of several films is measured, all the other film thicknesses must be accurately known prior to being able to measure the thickness of the film of interest.

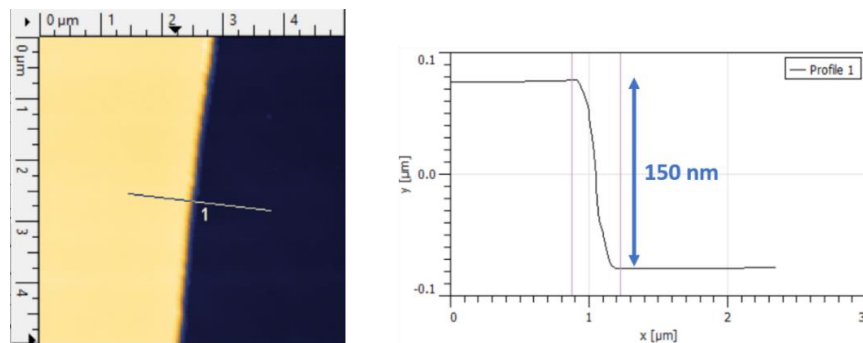


Figure 9 Left: An atomic force microscope image of a scratch for measuring the film thickness. An area of $5 \times 5 \mu\text{m}^2$ was scanned. Right: A depth profile over the edge of the scratch showing the determination of the film thickness. Images are screenshots from Gwyddion software.

2.3.3 Improving resist adhesion

Good adhesion of resists to the substrate is extremely important in achieving uniform and repeatable films by spin-coating. The main factor determining the adhesion between the resist and the substrate is that the surface energies of the two are matching. For example, resists with low surface energy stick best on a surface with low surface energy (i.e. a hydrophobic surface). A typical example of a low surface energy polymer is PMGI. See section 3.1.3.1 for improving the adhesion of PMGI on surfaces via HMDS treatment.

Most resists mentioned in this handbook have high surface energies, however, and thus stick best on surfaces with high surface energies (i.e. that are hydrophilic). A clean silicon surface (i.e. the native oxide layer) is naturally somewhat hydrophilic but we recommend increasing the substrate's surface energy wherever possible by one of the methods listed below (in decreasing order of observed effectivity):

- 1: Treat the substrate by oxygen plasma in a barrel asher (e.g. PVA TePLA barrel asher, 1 minute at 200 W power). Note that oxygen plasma may damage some substrates or materials deposited on them (e.g. graphene).
- 2: Bake the substrate on a hot plate at 200 °C for 5 min (= dehydration bake to remove the water molecules adsorbed on the surface).
- 3: Place the sample on a spin-coater chuck and dispense some (pure) solvent of the resist you want to coat the sample with (e.g. anisole). Let the solvent stand on the sample for 1 minute. Start the spinner (e.g. 4000 rpm, 40 s) to dry the sample. Coat with resist immediately once the chuck stops and start the spin-coating process.

3 Standard NanoFrazor processes

3.1 Bilayer lift-off

This chapter presents in detail the bilayer lift-off process which is probably the most straightforward method of transferring geometries patterned by the NanoFrazor into evaporated films of materials.

3.1.1 Introduction to bilayer lift-off

Bilayer lift-off (BLO) is an easy and quick process that is particularly well suited for deposition of metal contacts and for work with sensitive materials such as nanowires and 2D materials. As it relies on isotropic wet development, the achievable resolution is somewhat design-restricted. Highest resolution of transferrable features is in the range of 50 nm, but with an optimized process and by using special geometries, even sub-10-nm gaps can be achieved.

This document provides example processes for bilayer lift-off using two different underlayer materials: PMGI and PMMA/MA. Please also see the "Bilayer lift-off for NanoFrazor lithography" application note for more application examples on the process. Furthermore, the SwissLitho team will be happy to assist with any questions you might have.

3.1.2 Lift-off resists and their properties

Two different lift-off resist materials, PMGI and PMMA/MA have been found to work very well for the bilayer lift-off process. They have some important differences when it comes to processing and these are summarized in Table 2 below.

Table 2 Properties of lift-off resists tested for bilayer lift-off with NanoFrazor.

	PMGI	PMMA/MA
Substrate pre-treatment	HMDS priming	O ₂ plasma
Soft-bake temperature	225 °C	180 °C
Thickness range	20 - 300 nm	20 – 500 nm
Solvent	Cyclopentanone + PGME	PGME <u>or</u> ethyl lactate
Developer	Base (TMAH in water)	Solvent (IPA/DIW or ethanol)
Stirring required?	No	Yes
Remover for lift-off	NMP or DMSO	Acetone or DMSO

3.1.3 Sample pre-treatment

For bilayer lift-off process to work well, the proper adhesion of the lift-off resist to the substrate is important. Some general recommendations are given in Section 2.3.3. in this document. For rendering hydrophilic surfaces hydrophobic and hence improving the adhesion of PMGI on them, use of HMDS is a very good option.

3.1.3.1 *HMDS adhesion promoter*

PMGI has a low surface energy and therefore sticks best on substrates with low surface energies (i.e. hydrophobic surfaces). The most common method of rendering substrates hydrophobic is to treat them with hexamethyldisilazane (HMDS). However, HMDS is a very toxic and highly volatile chemical that must be handled with extreme care. Most multi-user clean room facilities have specialized vacuum chambers and standard processes for treating substrates with HMDS. Evaporated HMDS provides a monolayer coverage of the sample and an optimal outcome. If no such setup is available, the following process may be used with proper safety precautions:

- 1: Heat the sample on a hot plate (180 °C, 5 min) to remove the moisture from the sample surface
- 2: Allow the sample to cool down for 30 s
- 3: Put the sample on a spin-coater and dispense HMDS over it using a pipette
- 4: Allow to sit still for 1 minute
- 5: Spin coat to remove the excess HMDS (the spin parameters can be the same as for PMGI later)
- 6: Add the PMGI and spin-coat normally.

Be very careful that you don't bring the liquid HMDS into close contact with the hot plate or the sample while it is still hot as the chemical is very volatile and will explode.

Important: we have observed that the HMDS treated samples (no matter how the HMDS was deposited) will become hydrophilic again in a few weeks' time. In this case, delamination of the resist from the substrate during developing may begin to occur.

3.1.4 Notes on patterning

Depending on the exact stack, substrate and desired pattern dimensions, the optimal tip heater temperature will be different. Here, we assume a 30 nm PPA layer on a 50 nm PMGI layer on a Si substrate.

Recommendations for optimal patterning:

- Start with a heater temperature of $\sim 950^{\circ}\text{C}$ and a target patterning depth of exactly (or a little bit more than) the PPA layer thickness (here: $\sim 32 - 35$ nm). This way, the closed-loop feedback of the NanoFrazor keeps the tip exactly at the interface of the PPA (top layer)/PMGI (underlayer), which helps to stabilize the patterning process.
- If you use smaller patterning depths (or temperature), the pattern depths might be too shallow and the PMGI is not fully exposed for the wet development.
- If patterned too deep (especially using other underlayers than PMGI), tip contamination will occur faster and tip lifetime will be reduced.
- As the tip gets older, you might need to increase the tip heater temperature to compensate for the reduced heat flux efficiency due to a contaminated tip.
- For higher resolution patterns ($< 50\text{nm}$ HP), it might be necessary to use lower tip heater temperatures ($< 950^{\circ}\text{C}$) as well as thinner PPA layers.

3.1.5 Descum, developing, lift-off

3.1.5.1 *Using a PMGI underlayer*

Polymethylglutarimide (PMGI) resist (SFG-S series from MicroChem) allows for spin-coating very thin films, starting from ~50 nm using SFG-2S. This resist also has a sufficiently low developing rate of ~1 nm/s required for reproducibly achieving a very high-resolution lift-off. PMGI sticks best on hydrophobic surfaces, so a pre-treatment of the surface with an adhesion promoter such as HMDS is recommended. As HMDS is highly toxic and volatile, we recommend the use of a dedicated HMDS priming setup (available in most clean rooms) for this purpose. HMDS pre-treatment also effectively prevents any water infiltration between the PMGI and the substrate and thus delamination of the resist film from the surface during development.

Spin curves for PMGI can be found on [the website of Kayaku Advanced Materials](#) (formerly MicroChem) and those for PPA can be found in Appendix 1. PMGI is baked on a hot plate at 200 °C for 1 min and PPA at 110 °C for 2 min. Typically, a minimum PPA film thickness of about 20 nm is required for a mechanically stable film that can support itself after the undercut has been formed in the developing step.

After patterning the PPA layer with the NanoFrazor, a short dry etch (an oxygen plasma ash) might be necessary for removing any residual PPA prior to the wet development of PMGI. As an example, a 5 s etch at 200 W power and with an oxygen flow of 400 sccm at 0.8 mbar (PVA TePLA tool) removes about 5 nm PPA – usually enough for achieving a clean lift-off.

For developing (i.e. dissolving) the PMGI, highly diluted tetramethylammonium hydroxide (TMAH) is used. The desired developing rate of 1 nm/s is obtained with a concentration of 0.17 mol/L and at this concentration the PPA remains unaffected by the developer up to several minutes. The required dilution 0.17 mol/L can be easily obtained from commercial TMAH based developers, e.g.:

10 mL **AZ326 MIF** + 5.6 mL H₂O or

17 mL **AR300-47** + 3.0 mL H₂O or

17 mL **AZ300 MIF** + 9.0 mL H₂O

For an even slower developing rate, 0.15 mol/L of TMAH develops the PMGI at about 0.3 nm/sec while dilutions with less than 0.15 mol/L TMAH do not develop the PMGI anymore.

It is generally recommended to somewhat "overdevelop" the sample to achieve a sufficient undercut. For example, for a 50-nm-thick PMGI film, developing the sample for 75-100 s results in an optimal outcome. After the developing step, the sample should be rinsed in pure water for a few seconds followed by a rinse in IPA for a few seconds. Finally, the sample should be dried in nitrogen flow. The sample is now ready for evaporation. A metal thickness of maximum 40 % of the PMGI thickness is recommended for a repeatable outcome. For lift-off, the PMGI can be dissolved in DMSO or NMP solvents (note that acetone does not dissolve PMGI). If the patterns are very small (i.e. the openings where the solvent can reach contact with PMGI are small), one can attempt to remove the excess

metal before the lift-off by pressing a piece of standard Scotch tape gently against the deposited metal film and removing it by pulling slowly from one corner. Most of the metal film should attach to the piece of tape and the solvent contact area is increased speeding up the polymer dissolution process. Mild ultrasonication while the beaker is placed in a water bath can also help in speeding up the process and in removing any residual metal flakes from the sample. At the end of the process, move the sample into isopropanol for about 30 s and dry it with a nitrogen gun.



3.1.5.2 *Using a PMMA/MA underlayer*

The PMGI resist layer can be replaced by PMMA/MA (AR-P 617 series, Allresist). There are some small differences in the properties and processing of PMGI and PMMA/MA which are outlined below.

Contrary to PMGI, PMMA/MA sticks best on hydrophilic surfaces. So a mild oxygen plasma treatment (e.g. PVA TePLA barrel asher at 100 W power for 1 min with 400 sccm O₂ flow at 0.8 mbar) is a suitable pre-treatment prior to spin-coating the resist. We recommend using PMMA/MA co-polymer from Allresist, available under the product name AR-P 617. Spin-curves can be found on [Allresist's web page](#). After spin-coating, the AR-P 617 is baked on a hot plate at 180 °C for 90 seconds. The PPA can be spin-coated directly on the AR-P 617 and baked for 2 minutes at 110 °C. Spin-curves for PPA are found in Appendix 1.

After patterning the PPA with the NanoFrazor, the AR-P 617 can be dissolved ("developed") using a mixture of deionized water (DIW) and IPA. The more DIW in the solution, the faster the developing rate will be. For a rate of around 1 nm/s, a solution with 5 v-% of DIW in IPA (e.g. 2.5 ml DIW + 47.5 ml IPA) can be used. Stir the mixture well before starting the developing to make sure the DIW and IPA are well mixed. Also, it is important to stir the sample during the developing to keep the develop rate constant over the entire developing time. Please note that the way you stir the sample during developing may affect the develop rate quite a bit. Here, by stirring we refer to holding the sample between tweezers and moving it in a circular motion within the developer mixture at a rate of about 1 s per round, alternating the direction of movement approximately every 10 s. Similar to PMGI, it is typically recommended to somewhat "overdevelop" the samples to obtain a well-defined undercut. For example, for a layer thickness of 50 nm and a develop rate of 1 nm/s, a recommended develop time would be in the range of 75-100 s.

Alternatively, for a completely water-free lift-off process, pure ethanol can be used for developing the PMMA/MA instead of an IPA/DIW mixture. The procedure is the same as for DIW in IPA but the developing rate for pure ethanol is approximately 1.8 nm/s. The rate can be further reduced by diluting the ethanol by IPA. Also for ethanol, stirring the sample during developing is very important.

After developing, rinse the sample in pure IPA and blow dry with N₂. Now the sample is ready for metal deposition. A metal thickness of maximum 40 % of the PMMA/MA thickness is recommended for a repeatable outcome. Suitable solvents for removing the PMMA/MA include acetone and DMSO. If the patterns are very small (i.e. the openings where the solvent can reach contact with PMGI are small), one can attempt to remove the excess metal before the lift-off by pressing a piece of standard Scotch tape gently against the deposited metal film and removing it by pulling slowly from one corner. Most of the metal film should attach to the piece of tape and the solvent contact area is increased speeding up the polymer dissolution process. Mild ultrasonication in a water bath can also help in speeding up the process and in removing any residual metal flakes from the sample. At the end of the process, move the sample into isopropanol for about 30 s and finally dry it with a nitrogen gun.

3.1.6 Notes on the possibilities and limitations of the process

Combining NanoFrazor lithography with the bilayer lift-off offers a very gentle nano- and microfabrication technique. Unlike other nanolithography methods, this combination avoids sample heating and damage by charged particles. As a result, it yields exceptionally good electrical contacts to sensitive 1D [3] and 2D [2] materials. However, undercut formation (see Figure 10) limits the resolution of this process: the minimum spacing between nearby features is restricted to around twice the thickness of the bottom resist layer.

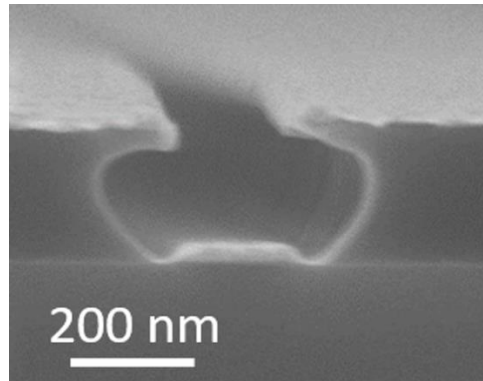


Figure 10 Cross section of a developed bilayer lift-off stack before lift-off showing the undercut.

Although the minimum feature separation of the bilayer lift-off process is limited, certain geometries allow for patterning of smaller gaps. For example, a design with two tapering electrodes produces a short suspended PPA bridge, which acts as a shadow mask during the evaporation process, producing sub-10-nm gaps between the electrodes (see Figure 11). The length of the gap is limited by the mechanical stability of the PPA bridge, which is likely to collapse with a length in excess of a few hundred nanometres.

Such ultra-narrow gaps are useful for fabrication of plasmonic bow-tie antennae or as quantum point contacts, for example.

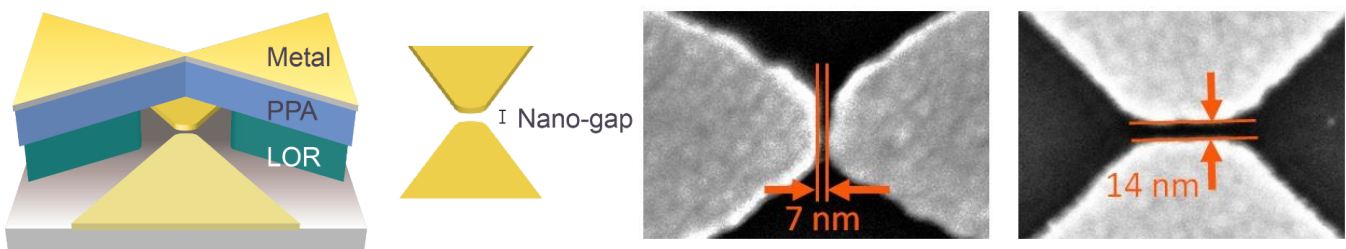


Figure 11 Suspended PPA bridge geometry enables the creation of very narrow gaps in between two metal electrodes.

3.2 High-resolution pattern transfer with a silicon hard mask

3.2.1 Introduction to high-resolution pattern transfer

NanoFrazor lithography can create patterns with resolutions down to the sub-10-nm range thanks to the extremely sharp tip used. However, due to the conical shape of the tip, the deeper the patterns are, the broader they become. Therefore, the shallower the patterning depth, the higher the achievable resolution is (see Figure 12 below). In order to take full advantage of the tip's sharpness, resist thicknesses of less than 10 nm must be employed. However, such thin layers are not practical for etching or lift-off processes by themselves but a multilayer process enabling pattern transfer from such a thin resist has been developed specifically for thermal scanning probe lithography at IBM Research – Zurich. [4]



Figure 12 The NanoFrazor tip is extremely sharp (left) but due to its conical shape the patterning depth influences the maximum resolution achievable (right).

In the process, the thin PPA layer is spin-coated on top of an ultra-thin inorganic hard mask (SH 113, PiBond Oy). A very thin layer (~2 nm) of PMMA can be added in between these two layers to act as a mechanical buffer and to increase tip lifetime by reducing mechanical contact between the sharp tip and the hard mask. At the bottom of the stack is a transfer layer. The material and thickness of this layer can be adapted depending on the intended pattern transfer process. The following two chapters describe the two most common high-resolution processes, lift-off and etching, in detail. Figure 13 shows a generic representation of a high-resolution pattern transfer stack.

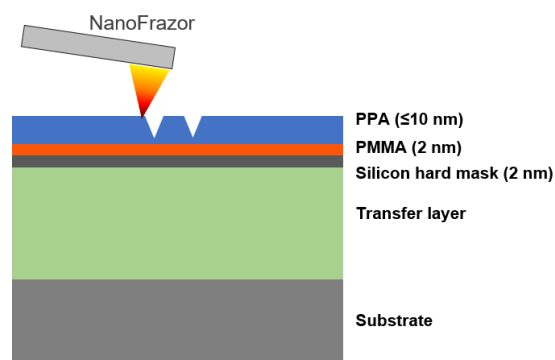


Figure 13 Resist stack used for high-resolution pattern transfer. Transfer layer thickness can be adapted according to application.

The pattern transfer process is carried out as follows (see Figure 14):

- 1: The thin PPA layer is patterned with the NanoFrazor. The maximum depth for the patterning is reached once the PMMA buffer layer is reached.
- 2: A descum process is carried out to remove any residual PPA and the PMMA buffer layer. A standard reactive ion etcher and N_2/O_2 etching chemistry is employed, see Appendix 3.
- 3: The patterns are then etched into the inorganic hard mask via reactive ion etching, using CHF_3 as the etching gas, see Appendix 3. As the hard mask layer is very thin, the thin PPA layer remaining after the descum process is enough to protect the unpatterned areas from etching.
- 4: Once the hard mask has been opened, the patterns can be etched into the transfer layer by reactive ion etching and O_2 as the etching gas, see Appendix 3. The hard mask layer is very resistant to oxygen plasma and etching through several hundred nm of transfer layer is possible, if necessary.

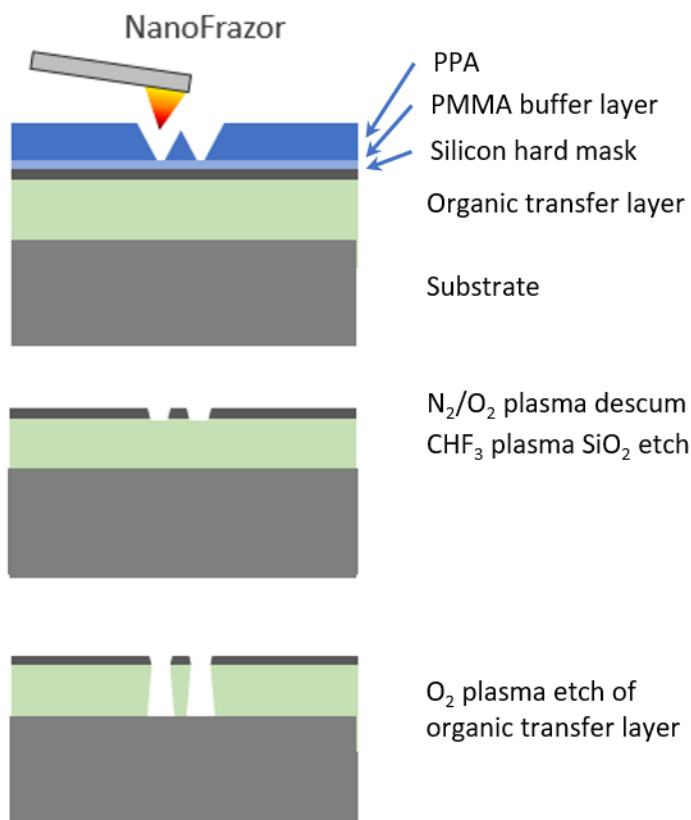


Figure 14 High-resolution pattern transfer stack patterning and etching process.

The following chapters go deeper into details for each of the steps mentioned above. Please refer to the application note "Ultra-High-Resolution Pattern Transfer for NanoFrazor Lithography" for more application examples on the process. Furthermore, the Heidelberg Instruments Nano / SwissLitho team will be happy to assist you with any questions you might have.

3.2.2 Sample pre-treatment

As for any nanofabrication process, the substrates should be as clean as possible before starting to prepare the pattern transfer stack. For standard silicon (or glass, quartz, sapphire) substrates we recommend the following sample cleaning procedure:

- 1: Place the sample in a beaker of acetone and the beaker in an ultrasonic bath for about 5 minutes.
- 2: Move the sample into a beaker of isopropanol (IPA) and continue ultrasonication for 2 minutes.
- 3: Dry the sample with a nitrogen gun.
- 4: Treat the sample with mild oxygen plasma. We use a PVA TePLA barrel asher for 1 minute at 100 W. Alternatively, a reactive ion etcher will also work. The main purpose of the oxygen plasma treatment is to render the surface of the sample hydrophilic for better resist adhesion rather than cleaning it.

If the substrates are sensitive to solvents or plasma treatment another applicable cleaning method may also be employed. Heating the sample on a hot plate (e.g. 5 minutes at 180 °C, i.e. dehydration bake) can be used to improve resist adhesion, but we have found oxygen plasma treatment to give the best results.

Sometimes PMGI (see Section 3.1.5.1) can also be used as a transfer layer for high-resolution processes. If using the material for this purpose, note that as an exception, PMGI prefers to stick on hydrophobic surfaces and a HMDS pre-treatment is recommended (see Section 3.1.3.1).

3.2.3 Preparation of the pattern transfer stack

All the layers in the high-resolution pattern transfer stack are prepared by spin-coating. The thicknesses of the layers, where necessary, can therefore be easily adjusted by varying the concentration and spin-speed of the material in question, see Appendix 1.

The typical thicknesses and spin-coating conditions for the different layers are as follows:

PPA:	10 nm (0.85 w-% PPA solution at 6000 rpm, bake 2 min at 110 °C), typical thickness range 8 nm (6000 rpm) – 15 nm (2000 rpm)
PMMA:	2 nm (1 part PMMA AR-P 672.02 from Allresist : 19 parts pure anisole, spin at 2000 rpm, bake for 1 min at 180 °C)
Hard mask:	1.5 nm (PiBond SH 113-10 at 5000 rpm, bake for 5 min at 180 °C, oxygen plasma in barrel asher at 200 W for 1 min, 400 sccm O ₂ , p = 0.8 mbar)
Transfer layer:	20 – 1000 nm (e.g. PMMA, OTL-405, PMGI, ...) → Refer to the spin-curves in Appendix I for spin-speeds and baking conditions.

3.2.3.1 Evaluating hard mask quality

The SH 113 hard mask (PiBond Oy) is a siloxane polymer that converts into an ultra-thin, pinhole-free material (essentially, silicon dioxide) once exposed to oxygen plasma after the spin-coating and soft bake. Even though the thickness of the formed layer is only in the order of 1.5 nm after the oxygen plasma exposure, the film is extremely smooth (r_{RMS} roughness typically ~ 0.3 nm) and pinhole-free. The shelf life of the product is one year when stored properly (in an airtight container at 5 °C). However, if the material is repeatedly taken out of the fridge and not allowed to warm to room temperature before opening, moisture from the ambient air will condense at the inside of the bottle and eventually mix with the material contaminating it and leading to unwanted artifacts in the spin-coated films.

In order to avoid the issue described above, we recommend aliquoting the material into e.g. glass vials with solvent resistant caps and only opening the “master bottle” when the material in the small vials runs out. The vials should still be stored at 5 °C but they warm up much faster and if any material degradation is detected (increased roughness, pinholes), the vial can be discarded and a new one introduced. We have found that by following the procedure outlined above, the shelf life of the SH 113 “master bottle” will reach one year while the vials should be replaced approximately every 3 months for optimal performance. As a rule of thumb, the time the bottle and the vials are kept at room temperature and with the cap open should be minimized.

In our experience, the most common sign of degradation of the SH 113 is the formation of pinholes, i.e. very small openings in the otherwise uniform film, see Figure 15a below. The pinholes can be detected by running a read-only scan of the high-resolution stack with the NanoFrazor (e.g. $5 \times 5 \mu\text{m}$ scan area with a 5 nm pixel size). The pinholes will be easily visible even after the thin PMMA and the PPA layers have been added on top of the hard mask, as in the images below. For comparison, Figure 15b below shows a high-resolution stack without pinholes. When pinholes are observed, we recommend replacing the SH 113 vial with a fresh one for the preparation of further samples.

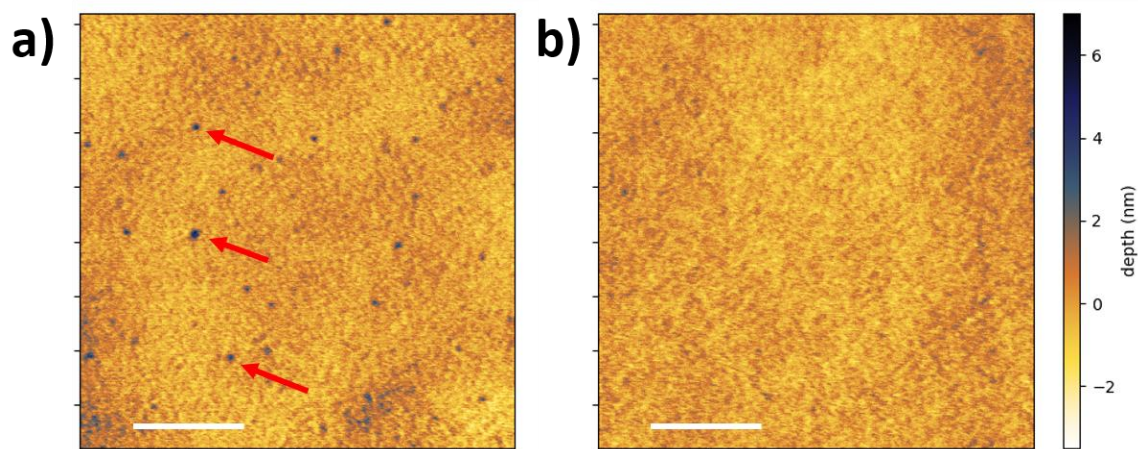


Figure 15 a) NanoFrazor image of a high-resolution stack with pinholes in the hard mask layer. b) A pinhole-free high-resolution stack. Scalebars are 500 nm.

3.2.3.2 *Notes on patterning high-resolution stacks*

Depending on the exact stack, substrate and pattern dimensions varying heater temperatures should be applied (here we assume 8-10 nm of PPA on a 2 nm PMMA on top of the silicon hard mask). Pixel size of 25 – 30 nm is generally sufficient.

Recommendations for optimal patterning:

- Start with an applied heater temperature of ~550-650°C (if the tip won't reach the sample surface, incrementally reduce the forward height down to about 200 nm).
- Use a target patterning depth of less than the top PPA layer thickness (here: 6 – 7 nm), otherwise you might hit the hard silicon hard mask and your tip gets blunted ("tip wear"). The ultra-thin PMMA layer in between the PPA and hard mask is recommended to prevent this.
- Try to use a calibration pattern consisting of patterns with varying widths in one design (ideally: 1px, 2px, 4px half-pitch, namely here: 25nm/50nm/100nm). The target is to achieve a homogeneous patterning depth of ~6 – 7 nm for all half-pitches.
- If the applied heater temperature is too hot, neighboring lines will merge together which leads to "recess" of the pattern and results in less available amplitude for subsequent dry RIE etching (narrow process window).
- If the applied heater temperature is too low, you will partially observe plastic deformation of your patterning resist (here: PPA) which leads to pile-up of material next to patterned structures.
- For some applications (for example line arrays) you even want to reduce the write pixel size in the fast writing direction (here: x). By decreasing the write pixel size, the heat flux per area is increased and lower temperature could be used.

3.2.3.3 Etching the PPA and the hard mask

Once the PPA on the high-resolution stack has been patterned, the resist stack needs to be opened by reactive ion etching. First, any residual PPA and the thin PMMA buffer layer are removed in a short descum process. The etching parameters we use are given in Appendix 3 as well as in Figure 17. The descum step typically lasts only 5-10 seconds, depending on the patterning depth and the thickness of the PPA used. For the resist stack opening, we use an Oxford Instruments PlasmaLab RIE 80 Plus system.

It is worth noting that in order to ignite the plasma reliably, an increased strike pressure (60 mbar) is used for the descum etch as opposed to the process pressure (15 mbar). This leads to an increased etching rate during the plasma ignition and stabilization phase at the beginning of the process, see Figure 16. The ignition phase of the etching process removes approximately 4.8 nm of PPA and the etch rate stabilizes to about 0.2 nm/s after that. Therefore, the amount of material consumed during the descum process can be approximated as follows:

$$\text{Thickness of material removed} = 4.8 \text{ nm} + 0.2 \text{ nm/s} \times \text{etching time (in s)}.$$

We note that even though this result is stable over time for a given RIE tool, it may be individual to the etch tool we have used for the experiment. Each etch tool has its own ignition behaviour, which should be verified case by case.

As the etching time is very short, it is recommended to observe the exact plasma ignition moment by eye through the observation window in the RIE etch chamber (see right on Figure 16). This is important as the plasma ignition (and hence the etching process) can start with a delay of up to 10 seconds from the moment when the instrument starts counting the time for the etching. If the user is not careful, this may result in severe non-uniformities in etching results.

Next, the SiO₂ layer is etched using CHF₃ chemistry. The selectivity of the etching process (Figure 17 or Appendix 3) is about 1:3 for PPA:SiO₂ while the hard mask etches at a rate of about 14 nm/min, so only a very thin layer of PPA is enough to protect the 1.5-nm-thick SiO₂ layer from being entirely etched. Typical etching times for the oxide etch process are in the range of 12 – 15 s. Also here, it is good practice to observe the ignition of the plasma carefully to ensure the repeatability of the etching times. The CHF₃ deposits on the chamber walls and easily mixes with the etching gases of the following etching steps, leading into unwanted etching of the oxide unless the sample is removed and the chamber

cleaned before. We have found a 5 min oxygen plasma cleaning step (40 sccm O₂, 200 W) to be sufficient to remove the residuals from the chamber and to ensure consistent results.

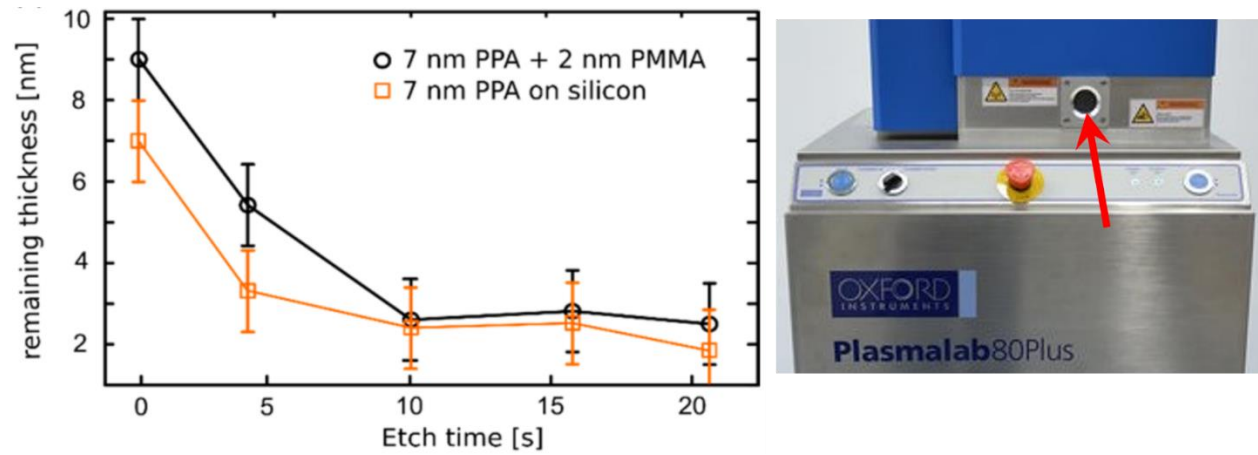


Figure 16 Left: Remaining material thickness as a function of elapsed time during the descum etch. [s]. Right: The exact moment of plasma ignition can be observed through the process monitoring window on the etching chamber.

3.2.4 High-resolution lift-off

3.2.4.1 *Opening the stack, lift-off*

We have adopted PMMA as the transfer layer for the high-resolution lift-off process as it is readily available in most clean rooms where electron beam lithography is performed. It also offers a favorable combination of properties for the process: a good etch selectivity against the inorganic hard mask material and solubility in acetone.

After the descum and hard mask opening steps, the PMMA still needs to be etched in a pure oxygen plasma etching process (parameters are given in Figure 17). The PMMA is etched at a rate of approximately 34 nm/min. It is worth pointing out that the substrate surface is in direct contact with the plasma once all the PMMA has been removed and using the process for work with materials sensitive to plasma should be carefully assessed. Refer to Chapter 5.4 for special considerations regarding working with 2-dimensional materials.

Once the stack has been etched open, the material to be patterned (e.g. metal) can be evaporated. The maximum thickness of the metal that can be easily lifted off has been experimentally found to be in the range of 60 % of the thickness of the transfer layer (PMMA) thickness.

As a final step, the transfer layer and the excess metal are dissolved by immersing the sample in a solvent. Both acetone and DMSO have been found to work well. Note that the openings where the solvent can contact the PMMA underneath the metal are typically very small and therefore dissolving all of the polymer can take a long time. In order to speed up the dissolution process, it is recommended to heat the solvent up, when possible to do so safely. When possible, leaving the sample in the solvent for a longer period of time, for example overnight, is advisable. The solvent DMSO is particularly recommended as it has a high boiling point and can be heated to higher temperature than acetone, for example. Mild ultrasonication in a water bath can also help speed up the process and to remove any residual flakes of deposited material from the sample.

At the end of the process, move the sample into isopropanol for about 30 s and dry it with a nitrogen gun.

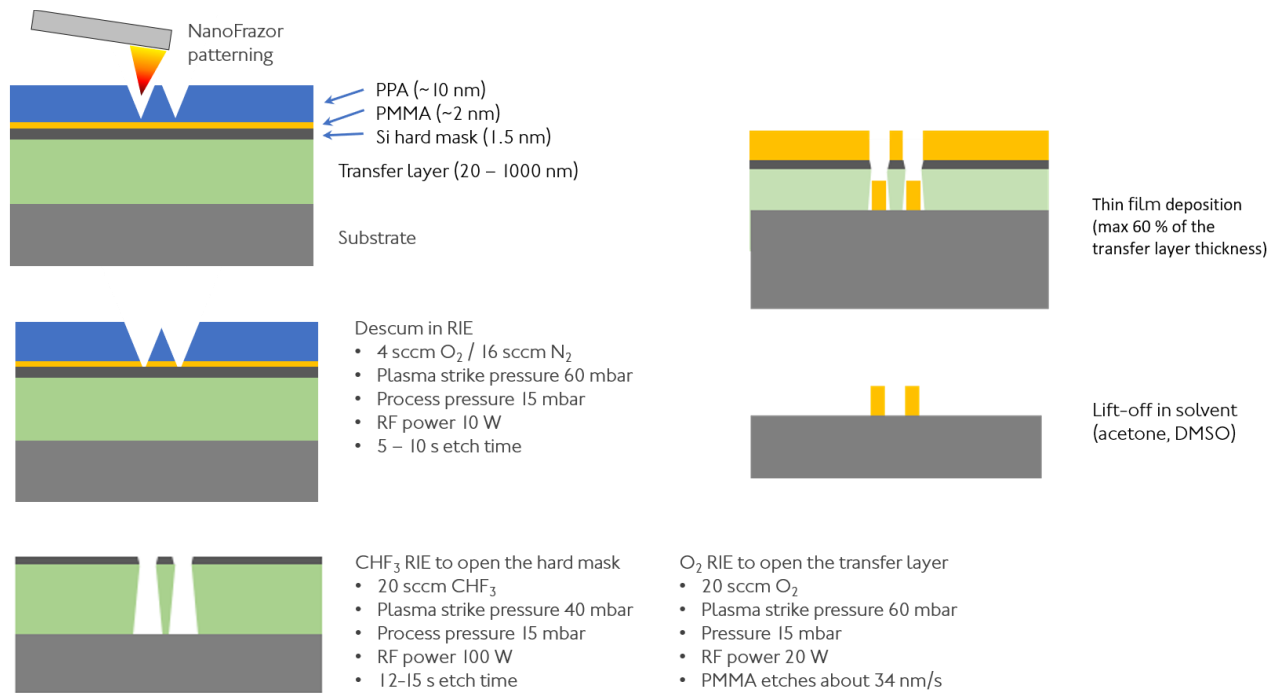


Figure 17 The process for high-resolution lift-off.

3.2.4.2 *Notes on the possibilities and limitations of the process*

High-resolution lift-off is a powerful and versatile process. Even though the layer thicknesses and etching times in the stack opening process have to be well controlled for a repeatable outcome, the process can be used very reliably.

A key parameter to consider is the PPA layer thickness. As described in Section 3.2.1, the thinner the PPA layer, the higher the resolution can be achieved. However, a minimum amount of PPA that can be removed in the descum process is in the order of 5-6 nm, setting an absolute lower limit for the PPA thickness. In fact, at the time of writing this document, the highest resolution nanostructures patterned with this process have been achieved with a 9-nm-thick PPA layer [4]. The larger the PPA thickness is compared to the minimum removed amount of PPA during the descum, the more buffer there is for the etching times and the more reliable the process is. However, a thicker PPA layer makes high resolution more difficult to achieve, causing a trade-off between reliability and resolution.

The transfer layer (PMMA) etch process is anisotropic but some degree of undercut is present, in particular if the etching process is longer than the PMMA thickness would require. Also, the etching rates are different for different RIE models and to some extent even with different RIE units, even if exactly the same parameters are employed. Therefore, calibrating the etch rate for the RIE to be used for opening the high-resolution stack is important. Also for this process, the initial plasma ignition step causes a distortion in the etch rate and we recommend measuring the etch rate as follows:

- 1: Coat 3 Si pieces with the same resist using exactly the same conditions.
- 2: Measure the film thickness on each of them (see Chapter 2.3.2).
- 3: Etch the three samples in three separate etch runs for 3 different times (e.g. 30 s, 45 s, 60 s)
- 4: Measure the film thickness for each sample and plot the reduction in film thickness against the etch time → the result should be a straight line the slope of which is the etching rate (note that the y-axis intercept gives the contribution of the plasma ignition)

If the structures to be etched are very narrow and long and close to each other (e.g. a line array), i.e. the aspect ratio (or the height divided by the width) is higher than ~4, pattern collapse might occur, see Figure 18. Modifications to pattern geometry might be necessary to overcome the issue.

$$\text{Tendency to pattern collapse} \propto A^2 = \left(\frac{H}{W}\right)^2/D$$

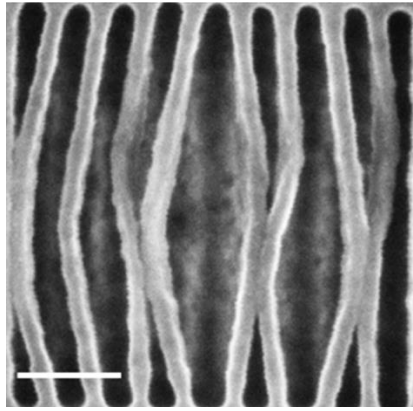


Figure 18 Pattern collapse in an array of lines that have been etched into a high-resolution stack. Here, the lines were too narrow, too close to each other and etched too deep to remain freestanding. Scale bar is 100 nm.

3.2.5 High-resolution etching

3.2.5.1 *Opening the stack, etching, removal of the stack*

After the descum and hard mask opening steps, the organic transfer layer (OTL 405) still needs to be etched in a pure oxygen plasma etching process (parameters are given in Figure 19 and in Appendix 3). Using this recipe, the OTL 405 is etched approximately at a rate of 20 nm/min.

Once the stack has been etched open, the patterns can be etched into the substrate. The maximum etching depth into the substrate is determined by the etching selectivity between the OTL and the substrate material. See Appendix 3 for selected etching selectivities.

In the end, the residual OTL 405 can be removed by mild oxygen plasma treatment (e.g. barrel asher) or with a Piranha solution.

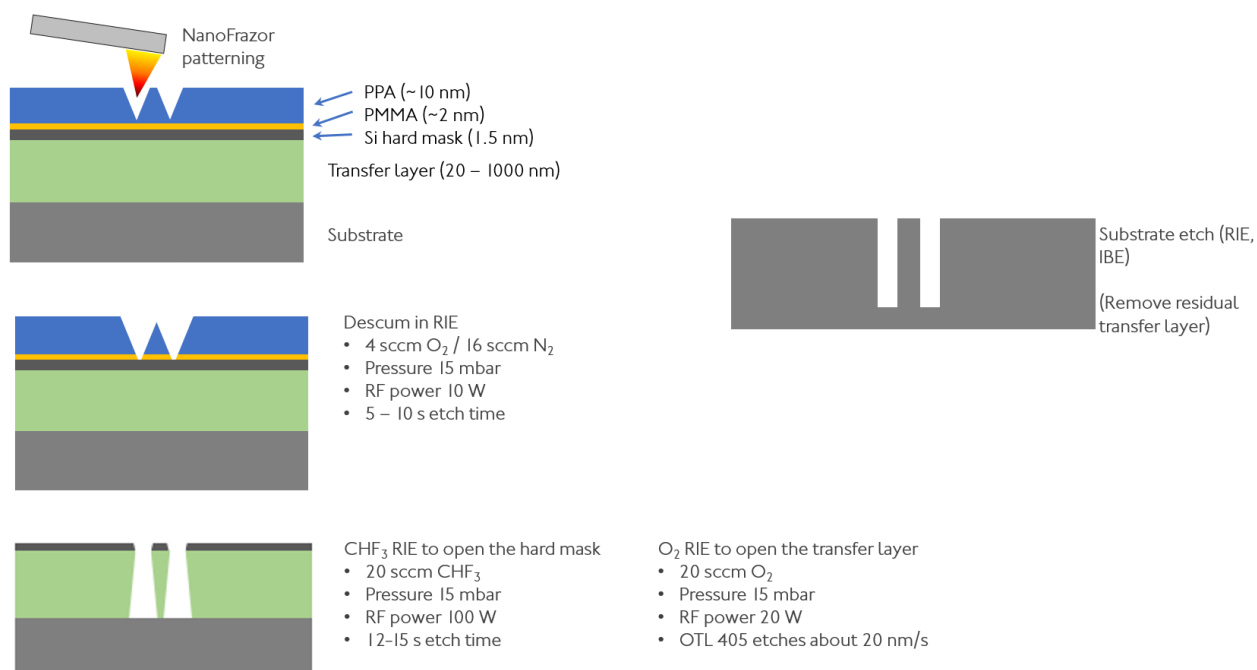


Figure 19 The process for high-resolution etching.

3.2.5.2 *Notes on the possibilities and limitations of the process*

High-resolution etching is a very powerful process and the highest resolution transfer of NanoFrazor patterns has been achieved using this technique.

Similar to the high-resolution lift-off process, the PPA layer thickness determines the maximum achievable resolution for the process, see Section 3.2.1 - the thinner the PPA layer, the higher the resolution that can be achieved. However, the minimum amount of PPA that can be removed in the descum process is in the order of 5-6 nm, setting an absolute lower limit for the PPA thickness. In fact, at the time of writing this document, the highest resolution etched nanostructures have been achieved with a 6.7-nm-thick PPA layer [5]. The larger the PPA thickness is compared to the minimum removed amount of PPA during the descum, the more buffer there is for the etching times and a more reliably process is possible. However, this also limits the achievable resolution.

The OTL 405 etch process is anisotropic but some degree of undercut is present, in particular if the etching process is longer than the OTL 405 thickness would require. Also, the etching rates are different for different RIE models and to some extent even with different RIE units, even if exactly the same parameters are employed. Therefore, measuring the etch rate for the RIE to be used for opening the high-resolution stack is important. See Section 3.2.5.2 for a recommended procedure of measuring the etch rate.

3.3 3D structuring resists & replication

3.3.1 Introduction to 3D pattern transfer

Due to the closed-loop-lithography (CLL) principle, NanoFrazor offers a uniquely high 3D patterning resolution, down to sub-nm regime. This capability has been demonstrated to enable the fabrication of new classes of devices [6-7] as well as to provide significant improvements to existing device concepts [8-9].

The NanoFrazor patterned polymer features can be used as functional components themselves [9], as masters for soft moulding or nanoimprint lithography [10] or by electroplating them into injection moulding templates [11]. Alternatively, the patterns can be etched into the material underneath the resist [8-9]. 3D structuring resists and the processes for 3D pattern transfer are described in detail below.

3.3.2 Some practical recommendations for 3D patterning

Depending on the exact stack, substrate and pattern dimensions different heater temperatures should be applied, pixel sizes of 25 - 50nm are most of the time sufficient for 3D patterning.

Recommendations for optimal patterning:

- Start with an applied heater temperature of $\sim 950^{\circ}\text{C}$. Make sure, you start with a reasonable forward height (distance between the tip apex and the surface), e.g. $\sim 300 - 400 \text{ nm}$.
- Turn the closed-loop feedback on (bowing correction off) and let it find a proper voltage range to pattern your design. You should roughly need 1 V per 100 nm of depth. If you are nearby the lower or upper limits of the applied electrostatic voltage (0 or 10 V respectively), adjust the forward height.
- Turn the bowing correction on once you are sure the pattern depths are appropriate for electrostatic forces in the regime of $\sim 3 - 7 \text{ V}$.
- As the tip gets older, you might need to increase the tip heater temperature to compensate for the reduced heat flux efficiency due to a contaminated tip.
- Keep in mind that you most often will not pattern down to your substrate (due to heat sink effect of the substrate) and a thin layer of undecomposed PPA will remain ($\sim 5-10\text{nm}$). Adding a thin PMMA thermal insulator layer underneath the PPA should allow for patterning a little bit deeper.
- Note that the shallower the pattern, the smaller the voltage range is assigned between individual depth levels and the relative error is increased. Therefore, 3D patterns with multiple depth levels and total target depths in the range of $< 10 \text{ nm}$ are very challenging to pattern.

3.3.3 Soft moulding from resist and nanoimprint lithography

Soft-moulding and nanoimprint lithography (NIL) are techniques where micro and nanometre scale structures are replicated via mechanical printing from a stamp template into a polymer layer. The soft-moulding refers to the fabrication of the first copy out of the structured resist, while NIL refers to the process of replicating the pattern into initially featureless material using the fabricated copy as a template (or a master). NIL in particular offers a cost-effective and scalable process for replicating complex 3-dimensional (3D) patterns onto a wide selection of substrates. Applications for such nanometre and micrometre scale, precisely crafted 3D structures include diffractive and refractive optical elements, other optical or photonics components, data communications, augmented/virtual reality (AR/VR) headsets and security features, with the potential to expand into the fields of biotechnology and nanofluidics in the future. NanoFrazor is very well-suited for the fabrication of defect-free and extremely precise 3D NIL master templates with sub-nm correspondence (i.e. 1σ error < 1 nm) between the target and patterned shapes having been demonstrated [8].

A possible process for UV-assisted soft-moulding and NIL process is presented in Figure 20 (a-f). First, the master template is fabricated by patterning the desired 3D structures into the resist (Figure 20a). Next, a working stamp (which is a negative image of the original pattern), is fabricated by casting a polymer precursor on the pattern. Depending on the materials combination used, treating the pattern surface with an anti-adhesion layer may be necessary to enable a clean release later. In the next step, a transparent back-plate is attached on top (Figure 20b). The working stamp is peeled off mechanically (Figure 20c) and the original master template can be reused for producing more working stamps, if desired. In the NIL process described here, the structures are replicated by pressing the soft and transparent working stamp against a liquid layer of nanoimprint resist followed by curing of the resist by exposure to ultraviolet (UV) light through the transparent back plate of the stamp (Figure 20d). Next, the working stamp is removed and an impression identical to the original patterns written in the master template is reproduced into the nanoimprint resist (Figure 20e). If desired, the working stamp can be moved to a new position on the substrate and the imprint and UV exposure process can be repeated arbitrarily many times (step-and-repeat NIL, Figure 20f) to multiply the area of the imprinted pattern. The benefit of the step-and-repeat approach is that the original pattern in the master template can be made smaller, thus significantly reducing fabrication costs. [10]

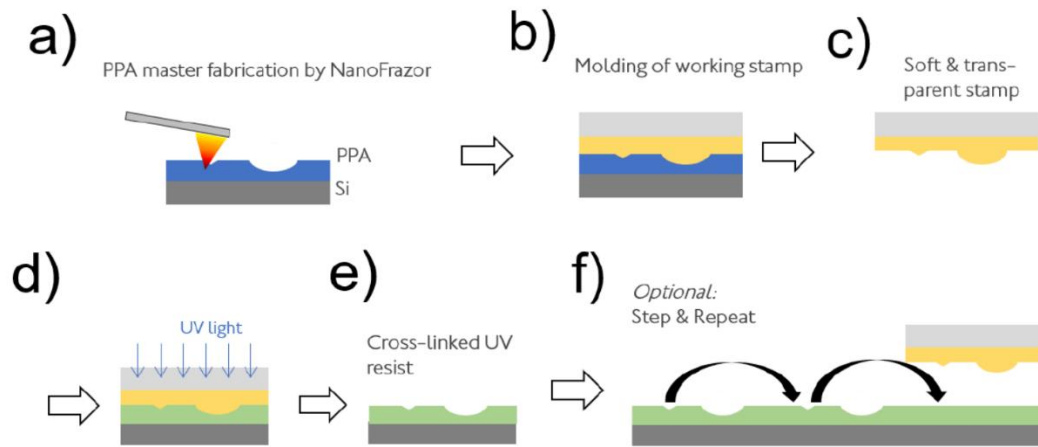


Figure 20 The main steps of the process for producing 3D replicas from a polymer master template. a) Writing the original 3D pattern into the thermal resist with the NanoFrazor, b) moulding a working stamp precursor material over the 3D shapes and attaching a transparent back plate, c) peeling off the working stamp, d) imprinting the pattern on the working stamp to a nanoimprint resist and curing by UV light, e) removal of the working stamp. Optionally, steps d) and e) can be repeated in a step-and-repeat process, (f). [10]

Figure 21 presents examples of nanoimprint lithography masters prepared by NanoFrazor and imprints prepared thereof. In Figure 21 a, an 8-level computer-generated hologram with a total depth of 64 nm written in PPA is shown while Figure 21 b shows the 10th imprint prepared from the pattern in Figure 21 a via the EVG SmartNIL[®] process. Figure 21 c shows an imprint prepared from a NanoFrazor pattern via a sol gel process developed at SCIL Nanoimprint Solutions. Figure 21 d shows two profile line scans measured over selected parts of c, demonstrating the high-resolution replication capability of the process.

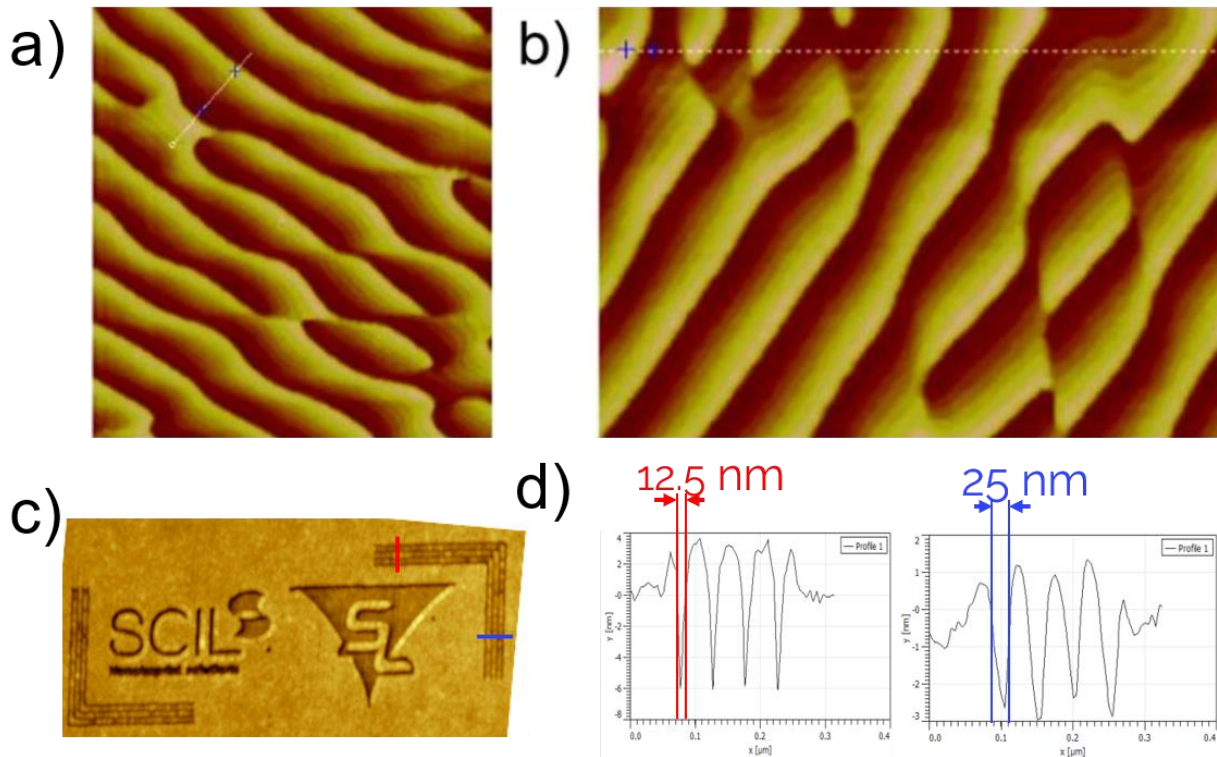


Figure 21 Examples of the nanoimprint lithography process with the masters prepared via NanoFrazor lithography. a) Atomic force microscope image of an 8-level hologram (total depth 64 nm) master in PPA. b) Atomic force microscope image of the 10th imprint prepared from the master in (a). (Images courtesy of EV Group) [10] c) Atomic force microscope image of a sol gel imprint prepared from a PPA master template. d) Profile scans across the red (left) and the blue (right) line in (c). Courtesy of SCIL Nanoimprint Solutions.

3.3.4 Replicating metals from 3D resist templates

This chapter presents approaches to reproducing 3D metal structures from NanoFrazor patterns. First, Rytka et al. [11] developed a metal electroplating process for fabrication of Ni shims for injection moulding of accurate 3D patterns. In their process (presented in Figure 22 a), the PPA patterns are first coated with a thin, yet continuous seed layer (e.g. Ti + Au) deposited by evaporation and then dipped in an electroplating bath where a current is passed through the solution until the desired thickness of metal (here, Ni) is reached. The PPA can be removed and the metal structure detached from the substrate by dissolving the PPA in a solvent such as acetone. An example electroplated structure (a topographic map of Switzerland) is shown in Figure 22 b.

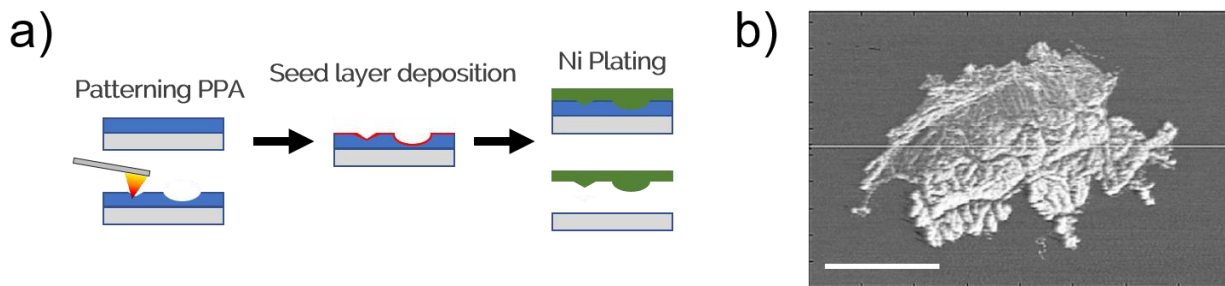


Figure 22 a) The process for preparing metal replicas from NanoFrazor patterns in PPA via electroplating. First, the 3D patterns are coated with a thin, conductive seed layer. The structures are dipped in a metal electroplating solution (here, Ni) and the electrodeposition process is applied until the desired thickness of metal is achieved. Finally, the metal is detached from the substrate by dissolving the PPA in a solvent. b) A topographical map of Switzerland prepared by Ni electroplating. The scale bar is 2 μ m.

Another way of reproducing nanometre-precise 3D metal structures out of NanoFrazor patterned polymer templates is template stripping (Figure 23 a) [6]. In the process, a 3D profile is patterned in a resist (here, PMMA/MA or CSAR were used, see Chapter 2.1.2). The depth of the patterns to be replicated were between 30 and 100 nm. Next, a relatively thick (> 500 nm) metal layer (here, Ag) is thermally evaporated directly over the patterned resist. Finally, a 1-mm-thick glass microscope slide is glued to the back of the metal layer with UV-curable epoxy adhesive and the glass/epoxy/metal stack is mechanically stripped off the polymer film. For more details, see Reference 6. A scanning electron micrograph of a 3D sine wave topography replicated into silver is shown in Figure 23 b.

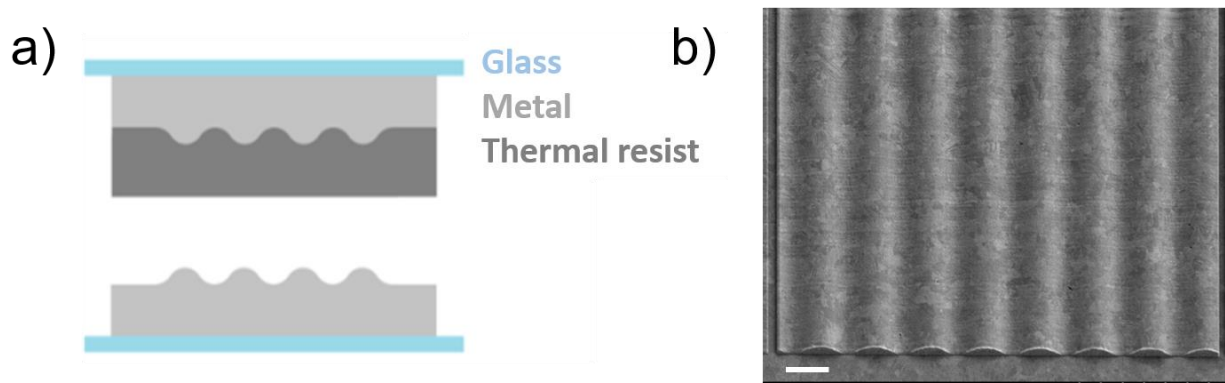


Figure 23 a) Template stripping process for replicating NanoFrazor patterned 3D topographies. A thick (> 500 nm) metal film is evaporated over the patterned resist and a glass slide is glued on it. The metal topography is mechanically stripped off the polymer film, producing a metal negative of the polymer pattern (b). The scale bar in the scanning electron micrograph is 2 μ m.

3.3.5 Notes on the possibilities and limitations of the process

Although 3D topographies can be very accurately patterned in resists with the NanoFrazor, the maximum patterning depth is limited to approximately 250 nm by the geometry of the tip. Deeper patterns can, however, be achieved by etching the polymer topography into the underlying substrate via reactive ion etching. The etching selectivity between the substrate and the resist will determine the pattern depth amplification factor. See Section 3.4 for further information.

It is worth paying attention to the compatibility of the pattern replication process and the master template (i.e. the patterned polymer resist) in terms of the:

- temperatures used (PPA, for example, becomes unstable at temperatures above ~110 °C)
- solvents and solutions casted over it (for a table on PPA's solvent compatibility, see Appendix 2)
- mechanical wear, e.g. while peeling the replica or the NIL master off the polymer film – the more force is required for this, the more damage to the patterned resist is likely to occur.

Again, transferring the patterns into the underlying substrate will provide a more robust and chemically stable platform for replication.

3.4 3D etching into hard materials

3.4.1 Introduction to 3D etching

Transferring 3D patterns from the resist into the substrate or other underlying materials has been demonstrated on several occasions and for several materials [6,8-10]. The principle is straightforward. First, a 3D pattern is structured into the resist material with the NanoFrazor. Second, reactive ion etching is employed for transferring the topography into the underlying material while the thermal resist acts as an etching mask that is slowly consumed during the process. The selectivity of the process, i.e. the ratio of the etch rates at which the resist and the substrate are consumed determines the amplification of the pattern depth. The main factors affecting the selectivity are the material combination chosen (e.g. PPA on silicon) and the etching chemistry and parameters.

This chapter describes the 3D etching processes in detail and gives practical advice for ensuring the best possible outcome for the process. However, as every application is different and as the model and usage history of the reactive ion etching tool play a big role in finding the right process conditions, careful calibration and testing are necessary for optimized results.

3.4.2 Reactive ion etching 3D structures into Si and SiO_x

The schematic for the 3D etching process is shown in Figure 24. The substrate should be as clean as possible before processing. We recommend carrying out the sample cleaning procedure described in Section 3.2.2 before spin-coating.

We have found that adding a thin (~2 nm) layer of PMMA (e.g. 1 part AR-P 671.02 : 19 parts anisole) underneath the thermal resist will act as a thermal buffer and a mechanical wear protection layer (orange layer in Figure 24). Adding this layer is not compulsory and PPA can also be spin-coated directly on the cleaned substrate. However, adding this buffer layer helps achieve a better pattern and higher uniformity especially for parts of the pattern closer to the substrate.

When it comes to the PPA thickness, a couple of considerations should be taken into account. First, we recommend adding a recess with a depth of 10 – 20 nm around the 3D topography to be patterned (Figure 24 a). The recess will provide additional flexibility for the etching time and will be explained in more detail below. Second, the NanoFrazor won't be able to remove the thermal resist all the way to the substrate surface. This is due to the fact that in the immediate vicinity of the substrate, the heat from the tip dissipates faster than within the "bulk" PPA, cooling the tip down and affecting the patterning. Therefore, one should always allow for a residual thickness of PPA in the order of 5 - 10 nm. Increasing the residual thickness is not recommended as this would prolong the etching time and could result in increased roughness of the patterns. The patterning depth depends on the etching selectivity of the process. Typical values for the patterning depth are in the range 30 – 100 nm. Finally, the required PPA thickness can be obtained by adding together the recess (10 – 20 nm), desired pattern depth (typically 30 – 100 nm) and the residual layer thickness (5 – 10 nm). Refer to Appendix 1 for the required PPA concentration and spin speed.

Selected reactive ion etching recipes for transferring 3D patterns are given in Appendix 3. As a rule of thumb, every reactive ion etching process has an ignition time when the plasma is ignited (typically at a pressure higher than that during the rest of the process) and when the etching rate is increased and nonlinear, see Figure 16 for an example. Ideally, the residual thermal resist layer and the thin PMMA buffer layer are etched during the ignition phase and the plasma has stabilized after about 5 – 10 s. The etch rate then drops significantly, approximately at the same time as when the substrate surface is exposed and the pattern begins to etch into it.

During the linear etch phase, both the thermal resist and the substrate material are consumed at rates determined by the material properties and the etching chemistry and parameters giving rise to selectivity and the maximal depth amplification achievable.

As determining an accurate etching rate or selectivity for an RIE process can be challenging (it depends on the proportion of the surface to be etched - the loading effect - as well as the usage history of the tool, for example) we recommend to introduce a recess in the pattern, as already mentioned above (see Figure 24 a). This recess provides some flexibility for the etching time. Ideally, the etching should stop exactly when the substrate surface under the recess is exposed and a thin residue of polymer remains outside of the recessed region (see Figure 24 b). However, in practice timing the etching this accurately is very challenging and therefore it is best to aim to

finish the etch halfway through the recess layer. Doing this will provide a window within which the etching time will be long enough to fully transfer the desired pattern to the substrate but not too long to damage the material around the recessed area. As the last step, the resist residues can be removed with oxygen plasma, with solvent or with Piranha cleaning.

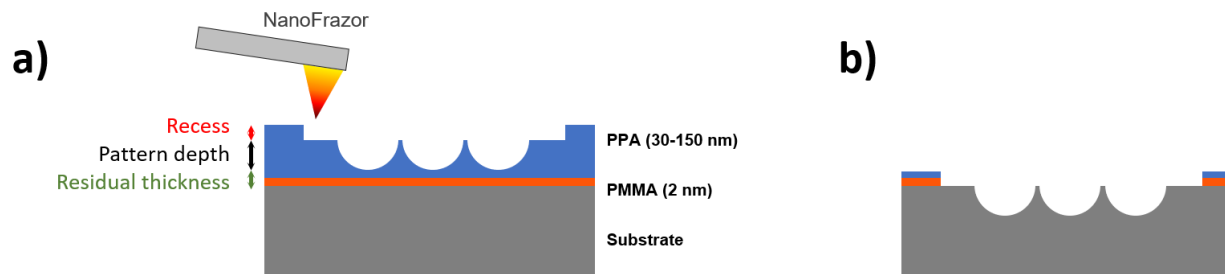


Figure 24 Schematic of a 3D etching process. a) The 3D pattern is written in the polymer with the NanoFrazor. The thin PMMA layer underneath the PPA provides a thermal isolation between the tip and the substrate. On the left of the schematic, the recess, pattern depth and the residual thickness are shown. b) The same pattern after an optimal etching depth has been reached: the substrate surface without pattern on top is not yet etched and a thin residue of polymer remains outside of the recess. The residues can be removed with oxygen plasma or with solvent.

Figure 25 shows an example of a 3D computer generated hologram topography in PPA (left) with a total depth of 64 nm transferred into the underlying silicon (right). Here, the total depth of the pattern transferred into silicon is 700 nm, corresponding to a depth amplification by a factor of > 10.

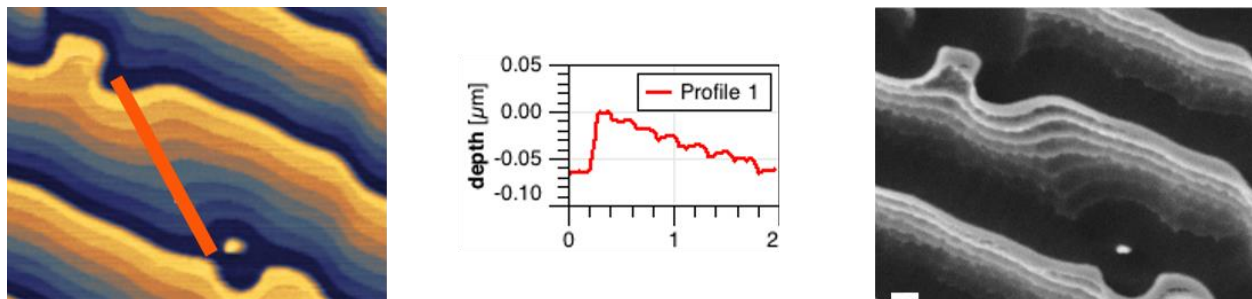


Figure 25 Computer generated 8-level hologram (left) with 8 nm individual depth levels and a total depth of 64 nm (see depth profile along the orange line in the middle image) was transferred into underlying silicon substrate (right). During the etching process, the total depth was amplified to 700 nm, corresponding to an amplification factor of ~11. The scale bar in the figure on right is 200 nm.

Finally, we note that due to the nature of the reactive ion etching process, in order to achieve predictable results in terms of etching rate, selectivity and surface roughness of the etched patterns it might be necessary to calibrate the tool each time before it is used. This is especially true if inconsistencies between separate etch runs are observed. Also, it is worth pointing out that the ignition of the plasma may be delayed by between 1 and 10 seconds after the process timer starts. This may lead into significant differences from run to run and we strongly recommend observing the real etching time (i.e. from the point when the plasma ignites) by paying attention to the timepoint of plasma ignition through the observation window in the process chamber, if available.

3.4.3 Amplified reactive ion etching with hard masks

With the patterning depth limited to a maximum of about 250 nm and the etching selectivity of PPA against silicon being about 10 at maximum, the practical maximum depth achievable using only a PPA etch mask is in the order of a few micrometres. However, the etching depth range can be extended by introducing an additional hard mask layer directly underneath the PMMA/PPA layer where the pattern is etched first before etching it into the desired substrate. The intermediate hard mask layer could be silicon dioxide [12] or the OTL 405 organic transfer layer, for example. Note that even though the example patterns given in this section are two dimensional, the process can also be applied to amplify the depths of 3D patterns.

In the amplification process, the desired topography is first patterned into the PPA layer (Figure 26 a). Next, the topography is etched into the intermediate hard mask in a reactive ion etching process (Figure 26 b). See Appendix 3 for suggested recipes for silicon dioxide etching. Note that achieving maximal amplification is not the aim of this process step but rather transferring the original topography into the intermediate hard mask as accurately as possible, including maintaining low surface roughness etc. Therefore, an etching selectivity of 1:1 would be optimal for this process. Finally, the pattern is etched into the substrate (e.g. silicon) in another reactive ion etching process (Figure 26 c). Here, the desired depth amplification is reached due to very good etching selectivity between the silicon dioxide and silicon. Pattern amplification by a factor of up to 100 for 2D patterns has been demonstrated with this method [12]. Figure 27 shows an example of a pattern that has been transferred into a silicon substrate using a silicon dioxide intermediate hard mask.



Figure 26 Process flow for amplified 3D etching. a) 3D topography is patterned in the PPA with the NanoFrazor. b) The pattern is etched first in the underlying hard mask via reactive ion etching. The selectivity of this process need not be high. c) Finally, the pattern from the hard mask is etched into the desired substrate material. The amplification of the pattern depth is mainly determined by the selectivity of this process step.

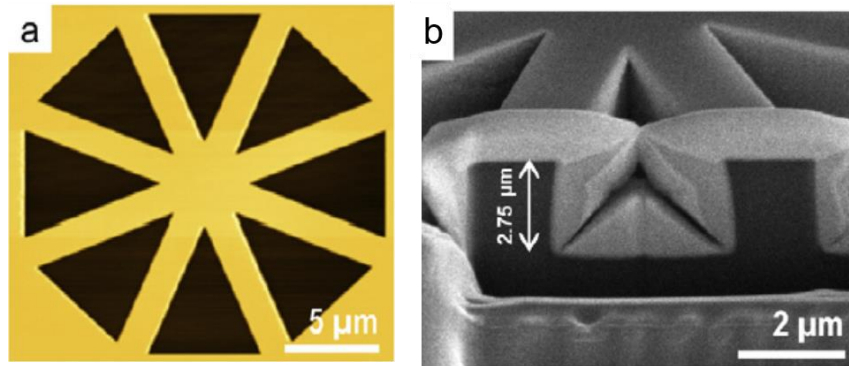


Figure 27 Example of depth amplification via an intermediate hard mask. a) NanoFrazor image of a 2D pattern in 102-nm thick PPA. The pattern depth is 82 nm. b) The pattern was etched into a 100-nm-thick silicon dioxide layer and further into the silicon substrate. The image shows a tilted (tilt angle 52°) scanning electron micrograph of a cross-section of the etched pattern with a total pattern depth of approximately 2.75 μm . The cross-section has been coated with a thick platinum layer (grey) before imaging. Adapted from Reference 12.

It should be noted that amplifying the depth of the pattern also amplifies the defects in it, including surface roughness although not necessarily by the same factor as depth. Several methods for reducing surface roughness (i.e. polishing) of etched 3D surfaces have been proposed, including exposing the etched surfaces to relatively mild ion bombardment, see Ref. [13] for more details.

4 Non-standard processes for pattern transfer

4.1 SIS – Sequential Infiltration Synthesis for high-resolution pattern transfer

A process resembling closely the high-resolution etching process described in Section 3.2.6 has been introduced in Ref. [14]. However, instead of using an ultrathin, spin-coated hard mask, the patterned PPA is converted into a hard mask in a gas infiltration process inside an atomic layer deposition chamber. The process is called sequential infiltration synthesis (SIS). The benefit of the approach is that it somewhat simplifies the process and allows for more flexibility in the thicknesses of the different layers employed.

First, the pattern transfer stack is prepared by depositing an inorganic transfer layer (here, silicon nitride, SiN_x) on a silicon substrate. (So far, the process has only been demonstrated on silicon substrates.) The thickness of this layer can be adjusted according to the desired final etching depth. Second, a buffer layer is needed to mechanically separate the PPA from the hard silicon nitride layer (cf. Figure 13). Here a cross-linked polystyrene is chosen, since it is inert to the process gases used in the infiltration process. Finally, a PPA layer (thickness ~10 nm) is spin-coated on top.

After patterning the PPA (Figure 28 a), the SIS process is carried out in a standard atomic layer deposition chamber at room temperature (25 °C) using trimethyl aluminium (TMA) and water as process gases. The process is a normal aluminium oxide growth process apart from longer cycle times and higher partial pressures that facilitate the infiltration of gases into the PPA film. During the process, the aluminium oxide forms within the bulk of the PPA forming a "composite" of carbon-carbon bonds and aluminium oxide with greatly improved etching resistance (Figure 28 b). After the infiltration the sample is exposed to unbiased oxygen/argon plasma (cf. barrel ash) in order to remove the residual organic contents from the infiltrated material. Next, the residual aluminium infiltrated PPA at the bottom of the pattern and the X-PS buffer layer are removed in an $\text{O}_2/\text{Cl}_2/\text{He}$ plasma etch process (Figure 28 c). The nitride is etched in a CF_4/CHF_3 RIE step to open the hard mask (Figure 28 d). Finally, the pattern is etched into the underlying silicon substrate by RIE using a $\text{CF}_4/\text{SF}_6/\text{N}_2$ gas mixture (Figure 28 e). An example of patterns with sub-10-nm transferred feature size is shown in Figure 29. Please refer to Ref. 14 for further details on the process.

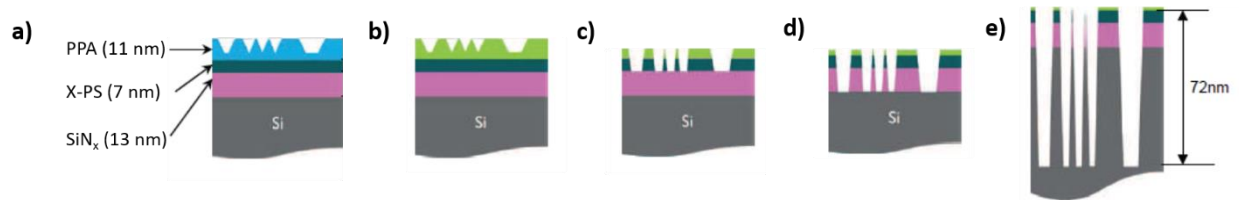


Figure 28 The sequential infiltration synthesis (SIS) process for high-resolution pattern transfer. a) The pattern transfer stack consists of a silicon nitride (SiN_x) film grown by chemical vapour deposition on the target substrate (here, silicon) and spin-coated cross-linked polystyrene (X-PS) and PPA layers. First, the PPA is patterned. b) SIS process is carried out by exposing the sample to Al_2O_3 growth precursors in a standard ALD chamber. c) A plasma descum process is applied to expose the silicon nitride layer below the pattern. d) The silicon nitride layer is etched to expose the silicon substrate. e) Finally, the pattern is etched into the silicon substrate. The silicon nitride provides a good selectivity for the etching and enables amplification of pattern depth. Adapted from Ref. 14.

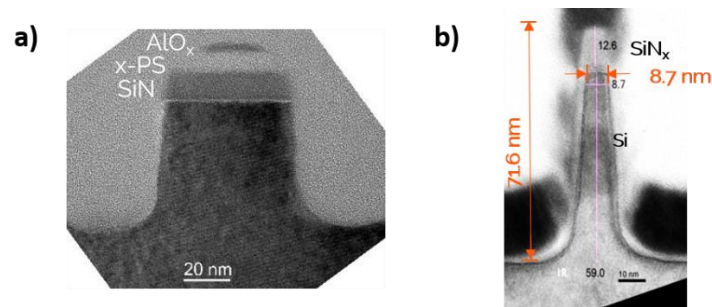


Figure 29 Example transmission electron micrographs of nanostructures fabricated via the sequential infiltration synthesis method. a) A cross-section of a line with the residual hard mask layers clearly visible and labelled. b) A nanopillar with a critical dimension of 8.7 nm. Adapted from Ref. 14.

5 Notes on relevant processing techniques and materials

5.1 Reactive ion etching

Reactive ion etching (RIE) is a very important pattern transfer process in micro and nanofabrication and very often employed for transferring patterns written by NanoFrazor lithography, in particular with either high-resolution lift-off or high-resolution etch processes. In general, the process can provide much better selectivity and anisotropy than wet chemical etching.

Perhaps the most important thing to keep in mind about RIE is that each tool has its own individual behaviour based on the model, age, usage history, etc. and therefore no universally working recipes can be provided. The recipes often must be somewhat adapted and the etching rates and selectivities calibrated for the local instruments.

Another important consideration (in particular for short etches) is that the plasma normally won't ignite on the exact moment when the process is started from the software but a delay of up to 10 seconds will occur. Therefore, we recommend observing the exact plasma ignition moment by eye through the observation window in the RIE etch chamber, see Chapter 3.2.3.3.

Etch rates of resists in oxygen plasma can be measured by following the procedure described in Section 3.2.5.2. For etching chemistries where the (silicon) substrate is also consumed, a new scratch must be made in the resist after the etching for measuring the residual film thickness. From the scratch made prior to the etch one can measure the sum of the depth of the etch into the substrate and the amount of resist consumed while the fresh scratch will allow for measuring the remaining resist thickness. In this way, both Δt_{resist} and $\Delta t_{\text{substrate}}$ can be measured and the etch rates and the etching selectivity can be calculated.

A selection of RIE recipes and supporting notes are given in Appendix 3.

5.2 Ion beam etching

Ion beam etching (IBE) has recently emerged as an alternative to conventional reactive ion etching technology, especially for applications where no suitable etch gases are available (e.g. etching noble metals). The process is always non-selective as it etches the sample via physical sputtering by argon ions and the process is mainly useful for etching relatively thin material layers. In general, polymers are more stable under Ar ion bombardment than metals and oxides but we have found that PPA is very unstable under ion bombardment and thus not suitable as a mask alone. However, our high-resolution etching stack has been demonstrated to work well with ion beam etching. See Figure 30 for an example.

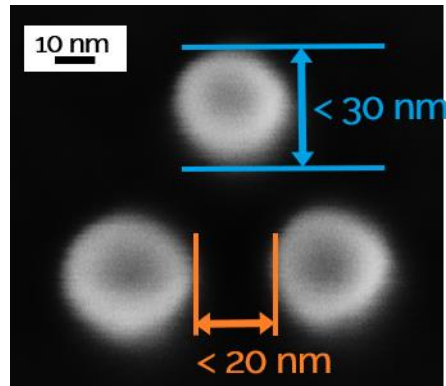


Figure 30 A plasmonic trimer etched in 20-nm-thick Au film by ion beam etching.

Table 3 *Recipes for etching gold and silicon in an Ionfab 300 tool (Oxford Instruments)*. below gives sets of parameters we have found to work for etching gold and silicon with a high-resolution etching stack. Note that exposure to Ar-ions tends to cross-link and carbonize the polymer transfer layer, making it difficult to remove it afterwards. Therefore, either a rather long oxygen barrel ash process or piranha are recommended for removing the remaining pattern transfer stack. Furthermore, applying a tilt and rotating the sample during the etching are important in order to avoid redeposition of the removed material and gradual narrowing of the patterns.

Table 3 Recipes for etching gold and silicon in an Ionfab 300 tool (Oxford Instruments).

	Gold etch	Si etch
Parameters	<ul style="list-style-type: none"> - Beam current: 250 mA @ 600 V - Acceleration voltage 390 V - Ar flow 10 sccm - Neutralizer current 550 mA - Neutralizer Ar flow 5 sccm - Platen temperature 5°C - RF Power: 1000 W - Tilt: 6° 	<ul style="list-style-type: none"> - Beam current: 300 mA @ 600 V - Acceleration voltage 390 V - Ar flow 10 sccm - Neutralizer current 550 mA - Neutralizer Ar flow 5 sccm - Platen temperature 5°C - RF Power: 1000 W - Tilt: 7°
Etch rates	<ul style="list-style-type: none"> - Au ~1 nm/s - OTL 405 ~1-3 nm/s 	<ul style="list-style-type: none"> - Si ~9 nm/min

5.3 Wet etching

PPA is in general not compatible with most concentrated acids and bases employed in fabrication of micro and nanostructures (e.g. sulphuric, nitric acid, potassium hydroxide, sodium hydroxide). It is very quickly consumed upon exposure to these chemicals. A notable exception, however, is buffered hydrofluoric acid (BHF) which can be used for short etch processes - it consumes PPA at a rate of approximately 10 nm/s. One application of BHF etching with PPA mask is fabrication of a sawtooth pattern as presented in Figure 31. In the process, the PPA is patterned, a short descum in a barrel plasma asher is carried out to expose the surface and the sample is dipped in BHF solution for a few seconds. Finally, the PPA is removed in acetone (Figure 31 a). As BHF etches the SiO_2 isotropically, a characteristic 3D groove shape is obtained, as shown in Figure 31 b. The pitch of the lines is 100 nm and the etched depth of the pattern is about 15 nm.

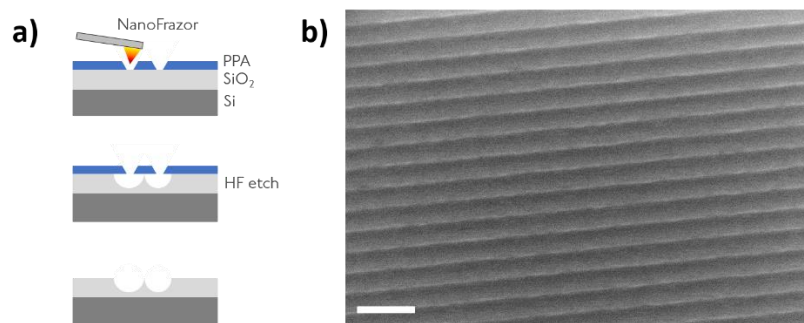


Figure 31 a) Process flow for BHF etching into SiO_2 with a PPA mask. b) Scanning electron micrograph of grooves etched into the oxide. The pitch of the pattern is 100 nm and the depth 15 nm. The scale bar is 200 nm.

5.4 Working with 2D materials

NanoFrazor lithography can be particularly powerful for fabricating devices out of 2D materials (e.g. molybdenum disulfide MoS_2 , graphene, hexagonal boron nitride h-BN, ...). For example, room-temperature Ohmic electrical contacts to MoS_2 were demonstrated [2]. One possible explanation for the exceptionally good quality of the contacts is seen in Figure 32 below: Figure 32 a shows how the material is very clean and undamaged after the resist on top was patterned by NanoFrazor and removed with a developer. In contrast, Figure 32 b shows the material after exposure to electron beam lithography and subsequent development – the material has residual polymer particles and the edges are notably rougher.

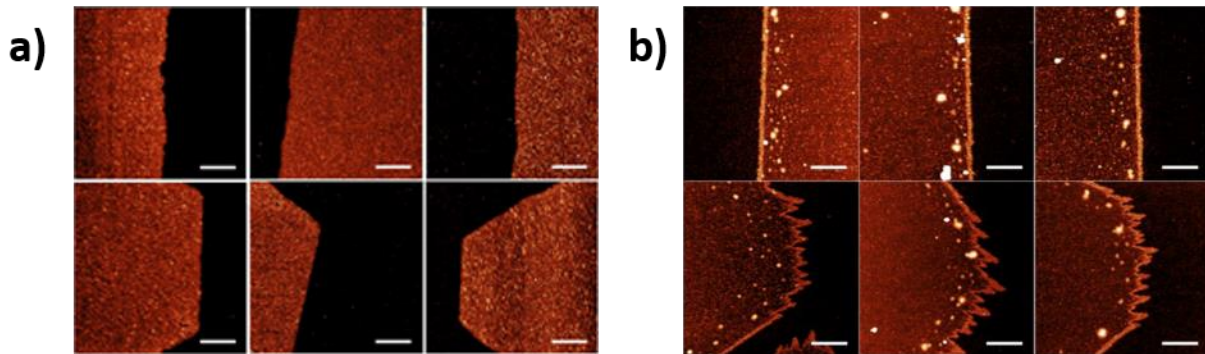


Figure 32 Atomic force micrographs of MoS_2 flakes after resist developing step. a) The patterning was carried out with a NanoFrazor. No residual polymer or modification of edges is observed. b) The material was patterned by electron beam lithography. Visible polymer residuals and increased roughness of the edges are seen. Scale bars are $0.5 \mu\text{m}$. Adapted from Ref. 2.

Furthermore, NanoFrazor is ideally suited for accurate overlay of electrodes over 2D material flakes (see Figure 33 a) via the bilayer lift-off process (Chapter 3.1). This is possible as the topography of even one-atom-thick materials is easily visible under a resist stack of up to few hundred nanometres thickness (see Section 2.3.1.1). Furthermore, etching 2D materials into desired shapes is possible by the high-resolution etch process (Section 3.2.6), as shown in Figure 33 b. MoS_2 readily oxidizes into a water-soluble oxide upon exposure to oxygen plasma and only a short rinse in deionized water prior to stack removal is necessary to remove the molybdenum oxide.

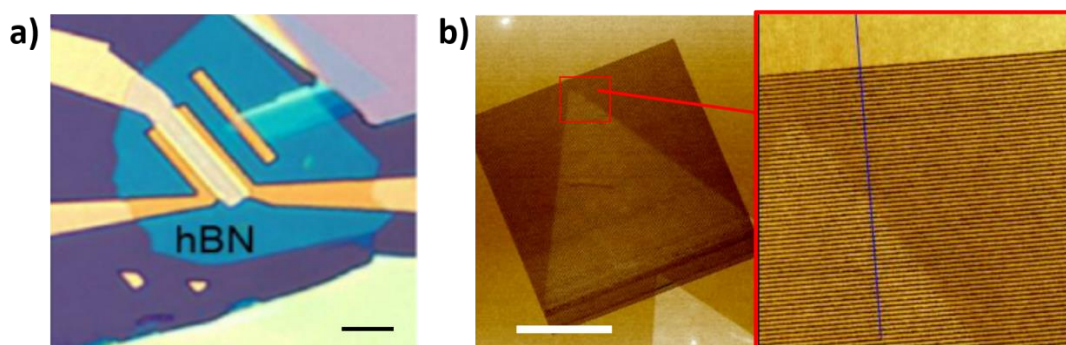


Figure 33 Examples of 2D material devices fabricated by the NanoFrazor. a) A top-gated MoS₂ transistor with h-BN top-gate dielectric where all the electrodes have been patterned with the NanoFrazor. [2] b) A chemical vapour deposited MoS₂ flake has been patterned with the NanoFrazor and etched into nanoribbons using reactive ion etching. Image courtesy of IBM Research – Zurich.

Certain 2D materials oxidize very easily or no exposure to humidity is desired when, e.g. stacking several 2D materials on top of each other. This being the case, NanoFrazor is a unique tool in that it can be used within a glovebox as no pumping or gas flows during its operation are necessary. In addition, the bilayer lift-off process can be carried out completely without exposing the samples to water (Section 3.1.5.2). Bilayer lift-off process is strongly recommended for 2D material work as no stack opening with plasma is required and thus possible damage to the sample is avoided. Also, no oxygen plasma treatment for resist adhesion promotion is recommended but the other methods listed in Section 2.3.3. should be employed, instead. In addition, we do not recommend facilitating the lift-off process by ultrasonicing the sample as this might remove or damage exfoliated 2D material flakes. Instead, we recommend using a pipette to apply gentle pressure over the sample surface during lift-off.

6 References

1. Rawlings, C. et al., *Accurate location and manipulation of nanoscaled objects buried under spin-coated films*. ACS Nano **9**, 6188–6195 (2015).
2. Zheng, X. et al., *Patterning metal contacts on monolayer MoS₂ with vanishing Schottky barriers using thermal nanolithography*. Nat. Electron. **2**, 17–25 (2019).
3. Wolf, H. et al., *Thermal scanning probe lithography (t-SPL) for nanofabrication*. 2019 Pan Pacific Microelectronics Symposium (Pan Pacific) 1–9 (2019).
4. Wolf, H. et al., *Sub-20 nm silicon patterning and metal lift-off using thermal scanning probe lithography*. J. Vac. Sci. Technol. B **33**, 02B102 (2014).
5. Ryu Cho, Y. K. et al., *Sub-10 nanometer feature size in silicon using thermal scanning probe lithography*. ACS Nano **11**, 11890–11897 (2017).
6. Lassaline, N., et al., *Optical Fourier Surfaces*, arXiv preprint arXiv:1912.09442.
7. Skaug, M. J., et al., *Nanofluidic rocking Brownian motors*. Science **359**, 1505–1508 (2018).
8. Rawlings, C. D. et al., *Control of the interaction strength of photonic molecules by nanometer precise 3D fabrication*. Sci. Rep. **7**, 16502 (2017).
9. Hettler, S. et al., *Phase masks for electron microscopy fabricated by thermal scanning probe lithography*. Micron **127**, 102753 (2019).
10. Kulmala, T. S. et al., *Single-nanometer accurate 3D nanoimprint lithography with master templates fabricated by NanoFrazor lithography*. Novel Patterning Technologies 2018, International Society for Optics and Photonics, 1058412, (2018).
11. Rytka, C., et al., *Iso- and variothermal injection compression moulding of polymer micro- and nanostructures for optical and medical applications*. J. Micromech. Microeng. **25**, 065008 (2015).
12. Lisunova, Y., et al., *High-aspect ratio nanopatterning via combined thermal scanning probe lithography and dry etching*. Microelectron. Eng. **180**, 20–24 (2017).
13. Lisunova, Y., et al., *Combination of thermal scanning probe lithography and ion etching to fabricate 3D silicon nanopatterns with extremely smooth surface*. Microelectron. Eng. **193**, 23–27 (2018).
14. de Marneffe, J.-F., et al. *Conversion of a patterned organic resist into a high performance inorganic hard mask for high resolution pattern transfer*. ACS Nano **12** (11), 11152–11160 (2018).
15. K.L. Camera et al., *Transient materials from thermally-sensitive polycarbonates and polycarbonate nanocomposites*. Polymer **101**, 59–66 (2016).
16. T. Sasaki et al., *Photoinduced depolymerization in poly(olefin sulfone) films comprised of volatile monomers doped with a photobase generator*. J. Polym. Sci. A Polym. Chem., **50**, 1462–1468 (2012).
17. S.T. Howell et al., *Thermal scanning probe lithography – A review*. Microsystems & Nanoengineering **6** (21) (2020).

18. C. Aso et al., Polymerization of aromatic aldehydes. II. Cationic cyclopolymerization of phthalaldehyde. *J. Polym. Sci. A Polym. Chem* 7 (2), 497-511 (1969).
19. H. Ito, C.G. Willson. Chemical amplification in the design of dry developing resist materials. *Polym. Eng. Sci.* 23 (18), 1012-1018 (1983).
20. M. Tsuda et al., Acid-catalyzed degradation mechanism of poly(phthalaldehyde): Unzipping reaction of chemical amplification resist. *J. Polym. Sci. A Polym. Chem* 35, 77-89 (1997).
21. M. Warner et al., Improvement in the transience and mechanical performance of flexible Poly(phthalaldehyde) substrates, *Polymer* 202, 122588 (2020).

Table 6 The thicknesses of PMGI SFG-2S at 3000 rpm spin-coating speed for selected dilutions in G-Thinner solvent. The samples are baked on a hot plate at 200 °C for 60 s.

	[rpm]	1:3 (v-%)	1:2 (v-%)	1:1 (v-%)	Pure
PMGI SFG-2S on silicon (PMGI:G-Thinner)	3000	10	15	20	50

Links to relevant resist data sheets:

PMMA AR-P 670 series: https://www.allresist.com/wp-content/uploads/sites/2/2014/03/allresist_produkinfos_ar-p610_englisch.pdf

PMMA/MA: <https://www.allresist.com/ebeamresists-ar-p-617/>

CSAR: <https://www.allresist.com/csar-62-ar-p-6200/>

PMGI: <https://kayakuam.com/products/pmgi-lor-lift-off-resists/>

PPA: <https://www.allresist.com/ar-p-8100-phoenix-81/>

Appendix 2: Solvent compatibility of PPA

Table 7 Solubility of PPA in selected solvents. 20 mg of PPA powder and 980 mg solvent were mixed. Solvents labelled in yellow show good solubility. Note that anisole is strongly recommended for preparing spin-coatable solutions of PPA.

	Name	Other names	CAS #	Boiling point (°C)	Immediate Observation	After 24 hours	After 4 days	After 1 week
1	2-methoxyethanol (toxic!)	Ethylene glycol-monomethyl ether (Methyl Cellosolve, methyl glycol)	109-86-4	124	Precipitates	Not Soluble	Not soluble	Not Soluble
2	1-methoxy-2-propanol	Propylene glycol monomethyl ether (PM, PGME)	107-98-2	118-119	Precipitates	Not Soluble	Not soluble	Not soluble
3	Ethyl lactate	Ethyl 2-hydroxypropanoate, 2-Hydroxypropanoic acid ethyl ester	687-47-8	154.5	Precipitates	Not Soluble	Not soluble	Not Soluble
4	1-methoxy-2-propyl acetate (MPA)	Propylene glycol monomethyl ether acetate (PGMEA)	108-65-6	145-146	Precipitates	Not Soluble	Partially dissolves	Completely dissolves
5	Ethylene glycol acetate (toxic!)	2-ethoxy ethyl acetate, 1-acetoxy-2-ethoxy-ethane, ethylene glycol monoethyl ether acetate, collosolve acetate	111-15-9	156	Precipitates, begins to dissolve after 5 minutes	Fully dissolved after 10 minutes	Fully dissolves	Fully dissolves
6	γ -butyrolactone	gamma-hydroxybutyric acid lactone	96-48-0	204-205	Almost dissolves	Fully dissolves	Fully dissolves	Fully dissolves
7	Chlorobenzene	Monochlorobenzene (MCB)	108-90-7	131	Almost dissolves	Fully dissolves	Fully dissolves	Fully dissolves
8	Methyl isobutyl ketone (MIBK)	4-methyl-2-pentanone	108-10-1	114-115	Precipitates	Not Soluble	Not soluble	Not soluble
9	Methyl ethyl ketone (MEK)	Butanone, Butan-2-one	78-93-3	80	Partially dissolves	Partially dissolves	Partially dissolves	Partially dissolves
10	Tert-butyl methyl ether	Methyl tert-butyl ether (MTBE), 2-methoxy-2-methylpropane	1634-04-4	54-56	Precipitates	-	-	-
11	Ethylbenzene		100-41-4	136	Precipitates	Not Soluble	Not soluble	Not Soluble
12	Butyl acetate	Acetic acid n-butyl ether	123-86-4	126.5	Precipitates	Not Soluble	Not soluble	Not Soluble
13	THF	Tetrahydrofuran, diethylene oxide, 1,4-epoxy butane	109-99-9	66	Fully dissolves	Fully dissolves	Fully dissolves	Fully dissolves
14	Isopropanol	2-propanol	67-63-0	82.4	Precipitates	Not Soluble	Not soluble	Not Soluble
15	Acetone	Dimethyl ketone, 2-propanone	67-64-1	56	Precipitates	Gelled	Gelled	Gelled
16	Toluene	Methylbenzene	108-88-3	110	Precipitates	Gelled	Gelled	Gelled
17	1,4-dioxane	1,4-diethylene oxide	123-91-1	101.4	Fully dissolves	Fully dissolves	Fully dissolves	Fully dissolves
18	Xylene	Dimethylbenzene	1330-20-7	137-144	Precipitates	Not soluble	Not soluble	Not Soluble
19	NMP	N-methylpyrrolidinone, 1-methyl-2-pyrrolidone	872-50-4	202	Almost completely dissolves	Fully dissolves	Fully dissolves	Fully dissolves
20	Chloroform	Trichloromethane	67-66-3	61	Fully dissolves	-	-	-
21	DMF	N,N-dimethylformamide	68-12-2	153	Fully dissolves	Fully dissolves	Fully dissolves	Fully dissolves
22	Cyclohexanone	Pimelic ketone	108-94-1	156	Precipitates, begins to dissolve after 5 minutes	Fully dissolved after 10 minutes	Fully dissolves	Fully dissolves
23	Dioxolane	1,3-dioxolane, glycol methylene ether, 1,3-dioxacyclopentane	646-06-0	74	Fully dissolves	Fully dissolves	Fully dissolves	Fully dissolves
24	DMAc	N,N-dimethylacetamide	127-169-5	166	Fully dissolves	Fully dissolves	Fully dissolves	Fully dissolves

Appendix 3: Selected reactive ion etching recipes, etch rates and selectivities

Table 8 Suggested etching parameters for opening high-resolution transfer stacks. The tool used was PlasmaLab RIE 80 Plus (Oxford Instruments).

	PPA descum	SiO ₂ etch	PMMA/OTL etch	Silicon etch
Parameters	<ul style="list-style-type: none"> - 4/16 sccm O₂/N₂ - P_{RF} = 10 W - 15 mTorr, strike @ 60 mTorr - Bias ~60 V 	<ul style="list-style-type: none"> - 20 sccm CHF₃ - P_{RF} = 100 W - 15 mTorr, strike @ 40 mTorr - Bias ~330 V 	<ul style="list-style-type: none"> - 20 sccm O₂ - P_{RF} = 20 W - 15 mTorr, strike @ 60 mTorr - Bias ~110 V 	<ul style="list-style-type: none"> - 50/15 sccm CHF₃/SF₆ - P_{RF} = 200 W - 15 mTorr, strike @ 60 mTorr - Bias ~500 V
Target	Expose the SiO _x layer	Etch open SiO _x mask	Etch pattern into PMMA/OTL	Etch pattern into silicon substrate
Time	About 5 seconds *	About 12 seconds *	Depends on layer thickness	Depends on layer thickness
Comments	Ignition dominates the amount of material removed.	CHF ₃ redeposits on chamber walls and an oxygen clean step should be carried out after the step.	SiO _x hard mask is very stable.	Anisotropic silicon etch recipe recommended by Oxford Instruments.
Etch rate	<ul style="list-style-type: none"> - PPA: 20 nm/min - PMGI: 6 nm/min - PMMA: 9 nm/min 	<ul style="list-style-type: none"> - SiO_x: 15 nm/min - PPA: 5 nm/min - PMMA: 3 nm/min 	<ul style="list-style-type: none"> - PMMA: 30 nm/min - OTL: 20 nm/min 	<ul style="list-style-type: none"> - OTL: 0.7 nm/s - Si: 1 nm/s

* Note that the etching is faster during the plasma ignition phase.

Table 9 Suggested etching parameters for transferring 3D patterns into substrates. Note that two different tools for transferring PPA patterns into Si were employed.

	PPA into silicon AMS200, Alcatel)	PPA into SiO ₂ or TaOx	SiO ₂ into silicon (depth amplification)	PPA into silicon (APS, SPTS)
Parameters	<ul style="list-style-type: none"> - 40/60 sccm SF₆/C₄F₈ - 1500/15 W Source/Chuck - 1.5e⁻² mbar 	<ul style="list-style-type: none"> - 40/60 sccm SF₆/C₄F₈ - 1500/15 W Source/Chuck - 1.5e⁻² mbar 	<ul style="list-style-type: none"> - 40/55 sccm SF₆/C₄F₈ - 1500/30 W Source/Chuck - 3 mTorr - Substrate 20°C 	<ul style="list-style-type: none"> - 10/30/175 sccm C₄F₈/H₂/He - 1200/300 W Source/Chuck - 4 mTorr - Substrate 10°C
Comments	Selectivity depends on etch duration, pattern design and tool condition → calibrate for a similar dummy pattern first		Support wafer material is important for etch rate and selectivity (SiO ₂ or Si), see "Selectivities"	Tool is located at EPFL's CMI clean room.
Selectivities ($\frac{\text{substrate}}{\text{mask}}$)	4 - 10	<ul style="list-style-type: none"> - 0.7 SiO₂ (40/60 sccm) - 0.85 SiO₂ (30/70 sccm) - 0.5 TaOx 	<ul style="list-style-type: none"> - 40 with SiO₂ substrate - 20 with Si substrate 	NA
Etch rates	<ul style="list-style-type: none"> - PPA: 2 nm/s - Si: 8 nm/s 	NA	SiO ₂ : 35 nm/min	NA

Table 10 Recipes for etching graphene and MoS₂ for PlasmaLab RIE 80 Plus (Oxford Instruments).

	Graphene	MoS ₂
Parameters	<ul style="list-style-type: none"> - 20 sccm O₂ - 20 W - 15 mTorr, Strike 60 mTorr - Bias 110 V - Time 20-60 sec/layer 	<ul style="list-style-type: none"> - 20 sccm O₂ - 20 W - 15 mTorr, Strike 60 mTorr - Bias 110V
Post-processing and stack removal	<ul style="list-style-type: none"> - short dip in HF - rinse in acetone/IPA - heat in N₂/Ar atmosphere (~500°C) to fully remove PPA residues 	<ul style="list-style-type: none"> - MoS₂ forms MoO_x which is soluble in water (short dip), rinse in IPA - rinse in acetone/IPA - heat in N₂/Ar atmosphere (~500°C) to fully remove PPA residues

Table 11 Selectivities of materials relevant to transferring NanoFrazor patterns in "PMMA/OTL etch" process from Table 8. Values are normalized to PMGI SFG-2S.

Resist	O ₂ Etch rate ratio
SH-113	<0.01
OTL-405	0.8
PMGI SFG-2S	1
CSAR 6200.04	1.0
PMMA/MA 617.03	1.2
PMMA 671.02	1.3
PPA (SAL/IDM)	3.3

Imprint

Editor:

Heidelberg Instruments Nano · SwissLitho AG
Technoparkstrasse 1 · 8005 Zurich · Switzerland
www.himt.ch · +41 44 500 38 00
info-nano@himt.ch
June 2020

Text and Design:

Dr. Tero Kulmala
Dr. Emine Çağın
Samuel Bisig

All rights reserved

